Meteoritics & Planetary Science 39, Nr 8, 1287–1305 (2004)
Abstract available online at http://meteoritics.org

The activity of chromite in multicomponent spinels: Implications for T-fO_2 conditions of equilibrated H chondrites

Ronit KESSEL,[1*] John R. BECKETT,[1] Gary R. HUSS,[2] and Edward M. STOLPER[1]

[1]Institute of Earth Sciences, The Hebrew University, Givat-Ra, Jerusalem, 91904, Israel
[2]Department of Geological Sciences and Center for Meteorite Studies, Arizona State University, Tempe, Arizona 85287, USA
[*]Corresponding author. E-mail: kessel@vms.huji.ac.il

(Received 4 April 2003; revision accepted 1 May 2004)

Abstract–Activities of chromite in multicomponent spinels with compositions similar to those of H chondrites were experimentally determined by equilibrating Pt-alloys with spinel at known temperature and fO_2. Our results are consistent with predictions based on the spinel solid solution model incorporated into the MELTS program. Therefore, we combined literature formulations for the activities of components in spinel, the ferromagnesian silicates, and alloys with measured and literature (bulk alloy) compositions of the meteoritic phases to constrain T-fO_2 conditions for the H-group chondrites Avanhandava (H4), Allegan (H5), and Guareña (H6).

$Log_{10}fO_2$ values based on the assemblage of olivine + orthopyroxene + metal are 2.19–2.56 log units below the iron-wüstite (IW) buffer for any equilibration temperature between 740 and 990 °C, regardless of petrographic type. Only lower limits on fO_2 could be determined from spinel + metal equilibria because of the extremely low concentrations of Cr in the alloys of equilibrated H chondrites (≤3 ppb). $Log_{10}fO_2$ values required by spinel + metal equilibria are inconsistent with those for olivine + orthopyroxene + metal if equilibration temperatures were at or above those inferred from olivine-spinel thermometry. This probably indicates that the closure for spinel + metal equilibria occurred under retrograde conditions at temperatures below ~625 °C for Allegan and Guareña and below ~660 °C for Avanhandava.

INTRODUCTION

The ordinary chondrites are classified into three chemically distinct groups, H, L, and LL, each of which is further subdivided into petrographic types from 3 (least equilibrated) to 6 (most intensely metamorphosed) based on textures and the degree of chemical homogeneity of the constituent phases (Van Schmus and Wood 1967). Constraining the metamorphic conditions experienced by these meteorites is fundamental to understanding the thermal, chemical, and structural histories of their parent bodies (e.g., Miyamoto et al. 1981; McSween and Labotka 1993; Bennett and McSween 1996; Young 2001). In addition to temperature, oxygen fugacity (fO_2) is a key measure of physical conditions during metamorphism: the presence of Fe-rich metal in ordinary chondrites requires reducing conditions, and increases in the ratio of oxidized to metallic iron from H to L to LL chondrites have long been used to infer corresponding increases in fO_2 (e.g., Fredriksson et al. 1968; Dodd 1969). In addition, variations in fO_2 within each chondrite group have been inferred based on systematic changes in the compositions and abundances of FeO-bearing phases (e.g., Fredriksson et al. 1968; Dodd 1969; Rubin et al. 1988; McSween and Labotka 1993).

In several studies, oxygen fugacity has been either calculated or measured explicitly. Based on these studies, there is general agreement that fO_2s during metamorphism of ordinary chondrites were below those of the iron-wüstite (IW) buffer, but the results are inconsistent in a number of important details. For example, Brett and Sato (1984) and Williams (1971b) obtained oxygen fugacities about one log unit below IW (IW – 1), while McSween and Labotka (1993) determined fO_2s of ~IW – 3. Differences at this level are significant and have a dramatic effect on the results of calculations of fluid evolution in the parent body (Hashizume and Sugiura 1997). The issue of whether these meteorites were open or closed with respect to oxygen during metamorphism is also unresolved. For example, based on intrinsic fO_2 measurements, Brett and Sato (1984) found that increasing intensity of metamorphism in equilibrated ordinary chondrites was accompanied by decreasing fO_2 relative to the IW buffer, while Walter and Doan (1969), McSween and

Labotka (1993), and Gastineau-Lyons et al. (2002) used geochemical arguments to support the idea that progressive metamorphism was characterized by increasing fO_2 relative to IW and increasing oxygen contents of the rocks. These proposed shifts in fO_2 and/or oxygen content are, however, subtle, and resolving which are correct requires accurate determinations of fO_2.

In this paper, we evaluate the conditions experienced by equilibrated H chondrites through application of olivine + orthopyroxene + metal and spinel + metal oxygen barometry. First, we determine chromite activities in spinels with compositions that approximate those in equilibrated ordinary chondrites using a technique developed by Kessel et al. (2003). Then we evaluate temperature-oxygen fugacity relationships in equilibrated H chondrites based on these activity-composition relationships for spinels, activity-composition relationships for other phases from the literature, and the compositions of coexisting phases in H chondrites.

METHODS

Starting Materials

Kessel et al. (2003) described an experimental method based on oxide + metal equilibration (following Chamberlin et al. 1994) by which the activity of chromite in multicomponent spinels can be determined by equilibrating spinels with Pt-rich alloys at controlled temperature and oxygen fugacity. In this study, we used this technique to determine the activity of chromite in multicomponent spinels with compositions that correspond to those in ordinary chondrites.

Six spinel end members (chromite [$FeCr_2O_4$], picrochromite [$MgCr_2O_4$], ulvöspinel [Fe_2TiO_4], qandilite [Mg_2TiO_4], hercynite [$FeAl_2O_4$], and spinel [$MgAl_2O_4$]) were synthesized from end member oxides. The synthesis procedures for chromite and picrochromite are described in Kessel et al. (2003). Ulvöspinel was prepared following procedures similar to those of Senderov et al. (1993): Reagent grade powders of Fe_2O_3 (JMC Puratronic) and TiO_2 (JMC Puratronic) were weighed out in the stoichiometric ratio and ground in an automated alumina mortar under ethanol for ~7 hr; the resulting mixture was pressed into 13 mm-diameter pellets, placed inside an alumina crucible, and suspended in the hot spot of a vertical furnace in flowing H_2-CO_2 gas at 1300 °C and $\log_{10}fO_2 = -10.5$ for 45 hr. Qandilite was prepared following the procedure of Sugimoto et al. (1997): reagent grade MgO (JMC Puratronic) was held in an alumina crucible in air at 1000 °C for 40 hr and then ground together with TiO_2 in the stoichiometric ratio in an automated alumina mortar under ethanol for ~6 hr; the mixture was then pressed into 13 mm-diameter pellets, placed inside an alumina crucible, and held at 1300 °C in air for 48 hr. Hercynite was prepared following the procedure of Petric et al. (1981): reagent grade powders of Fe_2O_3 (JMC Puratronic), Fe (Alfa® ÆSAR Puratronic), and Al_2O_3 (JMC Puratronic) were ground in stoichiometric proportions in an automated alumina mortar under ethanol for ~6 hr; the mixture was pressed into 7 mm-diameter pellets, placed inside loosely capped alumina ceramic cylinders, sealed inside an evacuated quartz tube, and then heated at 1100 °C for 4 days. Procedures for preparation of $MgAl_2O_4$ spinel were similar to those described in Mattioli et al. (1987): reagent grade MgO (JMC Puratronic) was heated in an alumina crucible at 1000 °C for 40 hr and then ground together with reagent grade Al_2O_3 (JMC Puratronic) in the stoichiometric ratio in an automated alumina mortar under ethanol for ~6 hr; the mixture was pressed into 13 mm-diameter pellets, placed on Pt foil inside an alumina boat, and inserted into a horizontal furnace for 48 hr at 800 °C in air; the furnace temperature was then increased to 1400 °C, and the sample was held at this temperature for an additional 48 hr.

Homogeneity of the products and the degree to which oxides were converted to spinel end members were determined using X-ray diffraction, scanning electron microscopy, and electron microprobe analyses of the synthesized spinels. The properties of the chromite and pichrochromite are discussed in Kessel et al. (2003). For two batches of ulvöspinel, the lattice parameter, a_o = 8.5126–8.5203 Å, is consistent with a stoichiometric ulvöspinel standard (8.5352 Å for NBS standard 25,20,61). The lattice parameters for two batches of qandilite, a_o = 8.4256–8.4351 Å (versus 8.4409 Å for NBS standard 25,12,25), one batch of hercynite, a_o = 8.1456 Å (versus 8.1534 Å for NBS standard 25,19,48), and one batch of spinel, a_o = 8.0811 Å (versus 8.08314 Å for NBS standard 25,9,25), are also consistent with literature data.

Figure 1 shows concentrations of picrochromite, hercynite, and $MgAl_2O_4$ spinel versus chromite content in spinels from H3–H6 chondrites based on data from the literature. Spinels in L and LL chondrites exhibit similar trends. The range of spinel compositions generally decreases with increasing petrographic type (e.g., 1σ on the mole fraction of chromite in spinels from H chondrites shown in Fig. 1 is 0.170 for H3, 0.027 for H4, 0.034 for H5, and 0.002 for H6), similar to what has been observed for olivines and pyroxenes in ordinary chondrites (e.g., Brearley and Jones 1998; Van Schmus and Wood 1967). No systematic shifts in average spinel composition were observed with increasing petrographic type, as is also the case for silicates in H chondrites (Brearley and Jones 1998).

Five spinel compositions were synthesized to capture the overall features of the observed compositional trend of spinels in H chondrites; these are shown as filled dark circles in Fig. 1, labeled OCa-OCe. One composition, OCa, is pure chromite, and the other four (i.e., OCb-OCe) are multicomponent spinels. The four multicomponent spinel compositions were

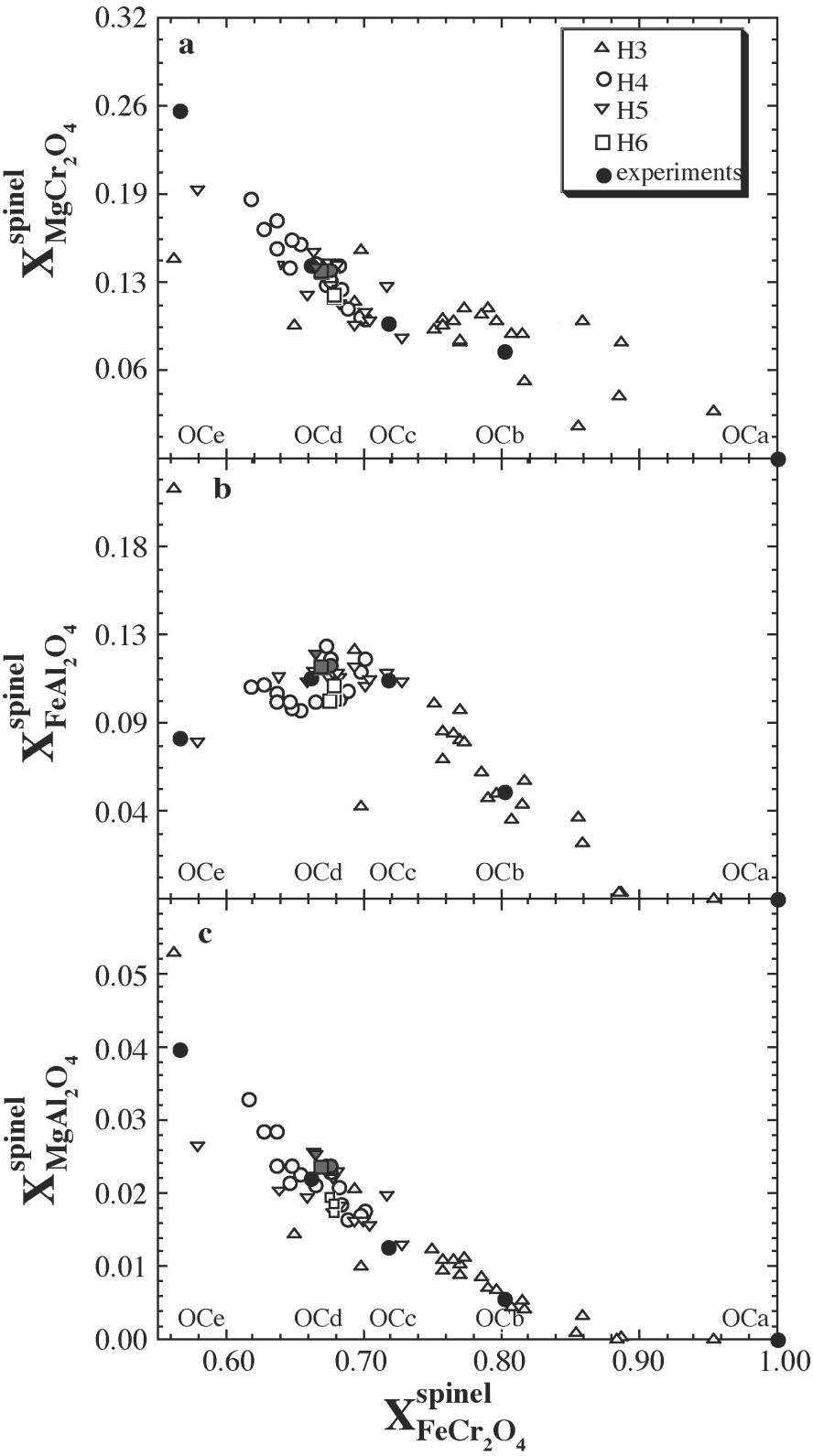

Fig. 1. Composition of spinels in H chondrites as a function of chromite content. Data sources: Buseck and Keil 1966; Bunch et al. 1967; Snetsinger et al. 1967; Keil and Fodor 1980; Bischoff and Keil 1983; Bischoff et al. 1989; Johnson and Prinz 1991; Ikeda et al. 1997; Zinovieva et al. 1997; Kleinschrot and Okrusch 1999; Kessel et al. 2004; and this study (gray filled symbols). Also shown (filled dark circles labeled OCa–e) are compositions of spinels used in the experiments: a) chromite-picrochromite; b) chromite-hercynite; c) chromite-spinel.

prepared by mechanically mixing the six spinel end members, described above, in appropriate proportions under ethanol for 2 hr using an automated alumina mortar. Each mix was then pressed into 13 mm-diameter pellets, placed inside an alumina crucible, and suspended from a sample holder at the hot spot of a vertical furnace in flowing H_2-CO_2 gas at 1300 °C and $\log_{10}fO_2 = -10.8$ (IW – 0.07). After 120 hr, the alumina crucibles were raised up in the gas flow into the cold region near the top of the furnace and allowed to cool. The pellets were taken out of the crucible and reground to produce the starting material used for the experiments. The homogeneity of the resultant starting materials and the degree to which the end members were converted to the desired spinels were determined using a Scintag Pad-V X-ray diffractometer and electron microprobe analyses. The spinel compositions, which agree within uncertainties with the target values, are reported in the columns labeled "Initial" in Table 1.

Experiments and Analytical Procedures

The experimental setup and calibration procedures are described in detail by Kessel et al. (2001, 2003). All of the experiments were conducted at 1300 °C and 1 atm in a Deltech DT-31 furnace or a home-built $MoSi_2$ furnace, both with gas-mixing capabilities. The oxygen fugacity was set by mixing CO_2 and H_2 and measured using an yttria-doped-zirconia solid electrolyte oxygen sensor ($SIRO_2$®, Ceramic Oxide Fabricators, Ltd., Australia) with an uncertainty of ±0.05 log units. Temperature was measured using a Pt-$Pt_{90}Rh_{10}$ thermocouple and is estimated to be accurate to within ±3 °C. In each experiment, seven crucibles made from 0.625 cm diameter, 10 mm long Al_2O_3 rods (Vesuvius McDanel) were suspended in the vicinity of the furnace hot spot. One crucible contained a pellet of Cr_2O_3 (6 mm in diameter, 1 mm thick) pressed around three pieces of pure Pt wire (3–5 mm long, 75 μm-diameter wire [99.9999%, Alfa® ÆSAR]). A second crucible contained a pellet of $FeCr_2O_4$ + Cr_2O_3, and a third contained a pellet of $FeCr_2O_4$. The results of experiments in these systems are given in Kessel et al. (2003) as part of a larger set of experiments and were used to model the thermodynamic properties of Pt-Fe-Cr alloys. Each of the remaining four crucibles contained two pellets of one of the synthesized multicomponent spinels, one of which was pressed around two Pt-Fe wires with Pt/Fe lower than expected for the equilibrium value, and the other was pressed around two wires with Pt/Fe higher than this expected value.

Experiments were conducted for 8–14 days to ensure equilibrium of the Pt-alloys with the surrounding oxides (see discussion in Kessel et al. [2003]) and were terminated by raising the crucibles into the cold region of the furnace under

Table 1. Compositions of experimental spinels.[a]

	OCb[b]			OCc			OCd			OCe		
	Nominal	Initial[c]	Final[d]	Nominal	Initial	Final	Nominal	Initial	Final	Nominal	Initial	Final
N[e]	–	9	28	–	9	28	–	9	25	–	9	28
FeO[f]	30.59	30.38(33)[g]	29.37(116)	30.18	30.16(223)	29.28(124)	28.60	29.39(45)	27.72(62)	24.17	25.38(33)	24.27(57)
MgO	1.78	1.68(3)	1.87(16)	2.40	2.20(43)	2.61(42)	3.62	3.50(34)	3.71(27)	6.55	6.37(45)	6.37(32)
Al_2O_3	2.83	3.27(66)	3.45(61)	5.93	6.01(92)	6.17(31)	6.51	6.49(92)	6.60(22)	6.03	5.97(33)	6.08(38)
Cr_2O_3	62.58	62.49(94)	63.32(121)	59.19	59.46(235)	59.83(89)	58.74	58.07(169)	59.63(51)	60.89	59.66(78)	61.09(53)
TiO_2	2.23	2.19(30)	1.99(29)	2.31	2.18(66)	2.11(27)	2.53	2.55(61)	2.34(33)	2.35	2.62(36)	2.19(29)
Cations per formula unit of 4 oxygens												
Fe	0.93	0.92(1)	0.89(3)	0.90	0.88(4)	0.87(2)	0.84	0.86(1)	0.81(2)	0.70	0.72(1)	0.70(2)
Mg	0.10	0.09(0)	0.10(1)	0.13	0.12(2)	0.14(2)	0.19	0.18(2)	0.19(1)	0.34	0.33(2)	0.33(2)
Al	0.12	0.14(3)	0.15(3)	0.25	0.25(4)	0.26(1)	0.27	0.27(4)	0.27(1)	0.25	0.24(1)	0.25(2)
Cr	1.79	1.79(3)	1.81(4)	1.66	1.67(7)	1.68(3)	1.63	1.62(5)	1.66(2)	1.66	1.63(3)	1.67(2)
Ti	0.06	0.06(1)	0.05(1)	0.06	0.06(2)	0.06(1)	0.07	0.07(2)	–	0.06	0.07(1)	0.06(1)
Mole fraction of end member spinel[h]												
Ulv	0.054	0.053(7)	0.047(6)	0.054	0.050(15)	0.047(6)	0.054	0.055(13)	0.048(8)	0.040	0.046(7)	0.038(5)
Chr	0.803	0.796(17)	0.787(14)	0.718	0.719(36)	0.707(18)	0.661	0.660(29)	0.647(22)	0.566	0.555(18)	0.560(12)
Her	0.054	0.062(12)	0.064(12)	0.109	0.108(14)	0.109(6)	0.110	0.110(15)	0.106(7)	0.081	0.083(5)	0.083(5)
PChr	0.078	0.078(2)	0.090(8)	0.100	0.095(18)	0.112(17)	0.140	0.140(11)	0.160(26)	0.253	0.253(15)	0.262(11)
Qan	0.005	0.005(1)	0.005(1)	0.006	0.007(2)	0.008(1)	0.012	0.012(3)	0.012(2)	0.020	0.021(2)	0.018(2)
Sp	0.006	0.006(1)	0.007(1)	0.013	0.015(4)	0.017(2)	0.022	0.023(4)	0.026(3)	0.040	0.038(4)	0.039(3)
Mgt	0.000	0.000(0)	0.000(0)	0.000	0.007(16)	0.000(0)	0.000	0.000(0)	0.000(0)	0.000	0.004(8)	0.000(0)

[a]Compositions are normalized to 100 wt%.

[b]OCb–e refer to the spinel compositions chosen to represent the composition trend in H chondrites as shown in Fig. 1. Data for OCa, which is pure chromite, are given in Kessel et al. (2003).

[c]Compositions of spinel after syntheses and before equilibration with Pt-alloys.

[d]Compositions of spinel after experiments. Values are average of analyses of oxides from one experiment for each run condition given in Table 3.

[e]Total number of analyses. Points were analyzed randomly on grains in the vicinity of the Pt-alloys.

[f]All Fe expressed as FeO.

[g]Numbers enclosed in parentheses indicate one standard deviation of the distribution of average grain compositions.

[h]Mole fractions of end member ulvöspinel (Uvl), chromite (Chr), hercynite (Her), picrochromite (PChr), qandilite (Qan), spinel (Sp), and magnetite (Mgt) were calculated based on mass and charge balance.

the flowing gas mixture. Once cooled, samples were removed from the furnace. A small piece of each pellet containing a Pt-alloy surrounded by oxides was mounted in epoxy to allow examination of oxide textures and compositions in the vicinity of the Pt-alloy. The second wire from each pellet was physically separated from the adjacent oxides and mounted such that a cross section of the wire was exposed. This sample was used to determine alloy composition and check for homogeneity across the wire. Alumina-impregnated papers were used to expose the wires and oxides, and diamond powder (<0.25 μm) was used to produce the final polished surfaces.

Phase compositions were determined using a JEOL733 Superprobe at Caltech following procedures described in Kessel et al. (2003). Spinels in the vicinity of the wires were analyzed for Fe, Cr, Ti, Mg, and Al, and Pt-alloys were analyzed for Pt, Fe, Cr, Ti, Mg, and Al. Magnesium (<40 ppm), Al (<30 ppm), and Ti (<100 ppm) in the alloys were below the detection limit in all experiments.

Meteoritic Samples and Analyses

In addition to our experiments, we studied three equilibrated ordinary chondrites: Avanhandava (H4), Allegan (H5), and Guareña (H6). All are unbrecciated falls characterized by low (≤S2) shock intensity (Grady 2000). The thin sections we examined (USNM 6882-1, USNM 953-2, and USNM 69-1, respectively) are the same thin sections included in the study of oxygen fugacity by H. Y. McSween and coworkers (2001, private communication). Four to seven contacting metal-spinel pairs in each thin section were located by SEM examination.

Silicates and Oxides

Olivine and pyroxene were always in contact with the spinel and metal grains. Spinel, olivine, and pyroxene were analyzed by electron probe using the same operating conditions used by Kessel et al. (2003). Spinels were analyzed for Fe, Cr, Mg, Al, Ti, Mn, Si, Ca, V, and Ni using Fe_2O_3, Cr_2O_3, $MgAl_2O_4$ (for both Mg and Al), TiO_2, Mn-olivine, anorthite (for both Si and Ca), V_2O_3, and NiO as standards. Silicon (<80 ppm), Ca (<120 ppm), and Ni (<430 ppm) were below detection limits. Olivines were analyzed for the same elements using fayalite, Cr_2O_3, forsterite (for both Mg and Si), anorthite, TiO_2, Mn-olivine, V_2O_3, and Ni-olivine as standards. Aluminum (<70 ppm), Ti (<260 ppm), Ca (<120 ppm), V (<270 ppm), and Ni (<430 ppm) were below detection limits. The same standards were used for pyroxene except that diopside was used for Si. Nickel (<430 ppm) and V (<270 ppm) were below detection limits.

The average compositions of spinel, olivine, and pyroxene are given in Table 2, and a compilation of all analyses is available from the authors. Olivine in all of the meteorites is forsteritic and the average mole fraction of fayalite (Fe_2SiO_4, Fa) of all grains analyzed in all the meteorites is 0.180 ± 0.003 (1σ). The dominant pyroxene is a low-Ca pyroxene; the average mole fractions of enstatite and wollastonite are 0.816 ± 0.003 and 0.0131 ± 0.0003 for the meteorites studied in this work. High-Ca pyroxene is present but rare. The chromite ($FeCr_2O_4$, Chr) contents of spinels in the H meteorites studied here are in the range 0.670 ± 0.005, similar in composition to the OCd synthetic multicomponent spinel (Fig. 1).

Metallic Phases

Most of the selected metal grains appear in the polished surface of the thin section as kamacite surrounded by spinel and silicates. However, SEM examination showed that one or two metal grains in each meteorite, although mainly composed of kamacite, have a thin taenite zone close to the rim, and one grain in Avanhandava was composed entirely of taenite.

Chromium contents of metal grains were analyzed using a Cameca IMS 6f ion microprobe at Arizona State University.

Table 2. Mineral compositions (wt%) in the equilibrated ordinary chondrites studied in this work.[a]

	Avanhandava (H4)			Allegan (H5)			Guareña (H6)		
	Olivine	Pyroxene	Spinel	Olivine	Pyroxene	Spinel	Olivine	Pyroxene	Spinel
N[b]	5/15	6/26	6/41	4/17	6/34	7/32	8/30	8/40	8/41
SiO_2	39.84(27)[c]	56.48(29)	B.D.L.[d]	39.65(61)	56.35(64)	B.D.L.	39.22(9)	56.05(15)	B.D.L.
TiO_2	B.D.L.	0.16(3)	1.54(13)	B.D.L.	0.19(1)	1.82(26)	B.D.L.	0.19(2)	2.02(14)
Cr_2O_3	0.04(3)	0.30(29)	57.00(43)	0.11(10)	0.36(17)	56.32(128)	0.31(29)	0.36(12)	56.86(47)
V_2O_3	B.D.L.	B.D.L.	0.71(2)	B.D.L.	B.D.L.	0.69(4)	B.D.L.	B.D.L.	0.70(3)
Al_2O_3	B.D.L.	0.31(26)	6.64(20)	B.D.L.	0.18(3)	6.90(59)	B.D.L.	0.17(1)	6.59(16)
FeO[e]	16.86(38)	11.05(41)	28.39(31)	16.07(22)	10.50(18)	27.76(32)	17.00(69)	11.23(8)	28.42(35)
MgO	43.25(21)	30.92(33)	3.21(19)	43.72(104)	31.10(55)	3.23(33)	42.45(56)	30.29(11)	3.24(21)
MnO	0.45(2)	0.50(1)	0.96(3)	0.47(2)	0.48(1)	1.01(4)	0.45(2)	0.50(2)	0.91(6)
CaO	B.D.L.	0.68(9)	B.D.L.	B.D.L.	0.70(4)	B.D.L.	B.D.L.	0.68(7)	B.D.L.
Total	100.44	100.40	98.45	100.02	99.85	97.73	99.43	99.47	98.74

[a]Individual results are available upon request from the authors.

[b]x/y refers to the number of grains analyzed (x) and the total number of analyses (y). Points were analyzed randomly in the central region of grains.

[c]Numbers enclosed in parentheses indicate one standard deviation of the distribution of average grain compositions.

[d]B.D.L. = below detection limit.

[e]All Fe expressed as FeO.

A focused O^- primary beam was used to sputter $^{56}Fe^+$ and $^{52}Cr^+$ ions from the metal grains in the carbon coated thin sections. A 20 × 20 μm area was first presputtered for 20 min with a 3 nA ion current to eliminate surface Cr contamination. Then, a 0.5 nA beam was focused in the center of the rastered area, masked by a field aperature, and the spot measured for 30 min. The secondary 0.07 ion mass spectrometer was operated at a mass resolving power of ~4800, sufficient to exclude contributions from $^{51}VH^+$ on ^{52}Cr and $^{55}MnH^+$ on ^{56}Fe. Data were corrected for electron-multiplier deadtime and a background count-rate of about 0.008 cps. Three Fe wires with Cr contents ranging from 100–976 ppm Cr, determined using the electron microprobe, were used as standards. Although the beam diameter was nominally 1–2 μm, the halo extended 10–15 μm away from the beam in all directions with intensity sufficient to contribute Cr ions from high-Cr phases. Thus, all data were collected at least ~20 μm from the edges of the metal grains. Traverses were taken across three kamacite grains in Allegan and Guareña. Rimming taenite was coarse enough to analyze in two grains from each meteorite. In Avanhandava, only kamacite (2 grains) was analyzed. The Cr content was found to be at or below the detection limit of ~3 ppb in all analyses from all three meteorites.

For metal in equilibrated H chondrites, it is the bulk composition at high temperature that is important for oxygen barometry because the coexisting kamacite and taenite compositions reflect later low temperature exsolution (e.g., Willis and Goldstein 1983). The bulk composition data of Jarosewich (1990) for the metallic fraction of unaltered equilibrated H chondrites average 9.6 wt% Ni; Afiattalab and Wasson (1980) obtained 10.2% Ni based on mass balance calculations; and Willis and Goldstein (1983) similarly estimated 10% Ni for metal from Guareña (H6), which is among the meteorites we studied. Bulk alloy compositions may increase during metamorphism by up to 0.5 wt% Ni (e.g., McSween and Labotka 1993), but this effect is within the error of determining the mean Ni content. For constraining the fO_2 prevailing close to peak metamorphic conditions, we assume a bulk concentration of 10 wt% Ni in the metallic phase. Since Cr contents are below the detection limit in both kamacite and taenite analyzed in the meteorites in this study, we assume an upper limit of 3 ppb Cr in the bulk metal phase at the closure temperature. Zanda et al. (1994) and Lauretta et al. (2001) inferred far higher concentrations of Cr in chondrule metal from unequilibrated chondrites (0.03–1.0 wt%), but these concentrations reflect the partitioning of Cr between silicate liquids and metal- and/or sulfide-rich liquids at higher temperatures during and immediately following chondrule formation in the solar nebula. Concentrations of Cr in metal from the equilibrated ordinary chondrites considered here refer to metamorphic conditions within the parent bodies as discussed below. The Co content in bulk metal in H chondrites is less than 0.5 wt% (Afiattalab and Wasson 1980), and as discussed below, its effects on Fe and Cr activities in the metal are small.

RESULTS

Activity-Composition Relationship of Chromite in Multicomponent Spinels

The experimental conditions and results for each set of experiments are listed in Table 3. Experiments were conducted at 1300 °C and 1 bar, with oxygen fugacities ranging from $\log_{10}fO_2 = -11.63$ to -9.22, which corresponds to −0.9 to +1.5 log units relative to the IW buffer. As described above, each of the two spinel-bearing pellets in each crucible was pressed around two Pt-Fe wires. One pellet in each crucible contained wires with an initial Pt/Fe ratio higher than the expected equilibrium value, and the other pellet contained wires with an initial Pt/Fe ratio lower than the expected equilibrium value. By starting with Pt/Fe ratios above and below the expected equilibrium alloy composition, we were able to bracket the equilibrium value by approaching it from two directions simultaneously.

The mole fractions of Cr and Fe in the alloys, X_{Cr}^{PtFeCr} and X_{Fe}^{PtFeCr}, were calculated from the measured wt% Cr and Fe by averaging three to five analyses done on the wires separated from the oxides in each pellet. The uncertainties were calculated as the standard deviation of the distribution of measured alloy compositions from each wire. The initial and equilibrium Pt-alloy compositions are given in Table 3. In ~60% of the cases, Pt-alloys at a given fO_2 and spinel composition converged to the same composition within 1σ, and all are within 2σ, giving us considerable confidence that equilibrium was closely approached during our experiments. The composition of spinel in equilibrium with each Pt-alloy was determined by analyzing spinels in the vicinity of the wires (Table 1). These "final" spinel compositions agree with the "initial" spinel compositions within 2σ, although Fe/Cr is consistently slightly lower.

The equilibrium between a Pt-Fe-Cr alloy and a Cr-bearing spinel in the presence of an oxygen-bearing vapor can be represented by the reaction:

$$Fe^{alloy} + 2Cr^{alloy} + 2O_2 = FeCr_2O_4^{spinel} \quad (1a)$$

The free energy of reaction for Equation 1a can be expanded in terms of component activities and solved for the activity of chromite in the spinel, $a_{FeCr_2O_4}^{spinel}$, yielding:

$$a_{FeCr_2O_4}^{spinel} = \exp(-\Delta G_1^o/RT)(a_{Fe}^{alloy})(a_{Cr}^{alloy})^2(fO_2)^2 \quad (1b)$$

In Equation 1b, a_i^j refers to the activity of component i in phase j, R is the gas constant, T is the temperature in Kelvin, and ΔG_l^o is the free energy of formation of $FeCr_2O_4$ from the elements. If ΔG_1^o, a_{Fe}^{PtFeCr}, and a_{Cr}^{PtFeCr} are known, then the

Table 3. Experimental conditions and results for Pt-Fe-Cr alloys + OC spinels at 1300 °C.

Run[a]	Spinel	X_{Fe}^{alloy}	X_{Fe}^{alloy} [b]	X_{Cr}^{alloy}	$\ln\gamma_{Cr}^{alloy}$ [c]	$\ln\gamma_{Fe}^{alloy}$	$a_{FeCr_2O_4}^{spinel}$ [d]	X_{Fe}^{alloy}	X_{Fe}^{alloy}	X_{Cr}^{alloy}	$\ln\gamma_{Cr}^{alloy}$	$\ln\gamma_{Fe}^{alloy}$	$a_{FeCr_2O_4}^{spinel}$
	Used	(Initial)	(Final)	(Final)				(Initial)	(Final)	(Final)			
$\log_{10}fO_2 = -11.63$, duration = 402 hr													
RK275-21	OCa							0.539(4)	0.510(1)	0.00572(3)	–2.25	–1.59(10)	0.98
RK276-21/45	OCb	0.408(3)[e]	0.575(2)	0.00187(1)	–1.58	–1.14(18)	0.71	0.539(4)	0.579(1)	0.00175(1)	–1.54	–1.11(19)	0.70
RK277-21/45	OCc							0.539(4)	0.556(2)	0.00230(2)	–2.59	–1.27(16)	0.61
RK278-21/45	OCd	0.408(3)	0.559(3)	0.00211(3)	–1.74	–1.25(16)	0.56	0.539(4)	0.558(3)	0.00208(1)	–1.76	–1.26(16)	0.53
RK279-21/45	OCe	0.408(3)	0.558(2)	0.00209(2)	–1.76	–1.26(16)	0.53	0.539(4)	0.556(1)	0.00215(1)	–1.77	–1.27(16)	0.54
$\log_{10}fO_2 = -11.20$, duration = 431 hr													
RK268-43	OCa	0.447(8)	0.479 (3)	0.00378(7)	–2.65	–1.88(7)	0.94						
RK269-21/43	OCb	0.447(8)	0.494(1)	0.00267(1)	–2.49	–1.76(8)	0.76	0.539(4)	0.499(2)	0.00240(2)	–2.42	–1.72(9)	0.75
RK270-21/43	OCc	0.447(8)	0.485(1)	0.00280(1)	–2.59	–1.84(8)	0.61						
RK271-21/43	OCd	0.447(8)	0.509(5)	0.00172(1)	–2.32	–1.64(10)	0.52	0.539(4)	0.517(2)	0.00157(2)	–2.22	–1.58(11)	0.56
RK272-21/43	OCe	0.447(8)	0.481(4)	0.00273(2)	–2.63	–1.87(7)	0.52	0.539(4)	0.492(1)	0.00225(1)	–2.51	–1.78(8)	0.51
$\log_{10}fO_2 = -10.61$, duration = 313 hr													
RK249-43	OCa							0.447(8)	0.426(1)	0.00268(2)	–3.34	–2.43(4)	0.95
RK250-43/44	OCb	0.371(3)	0.443(2)	0.00172(4)	–3.14	–2.26(5)	0.72	0.447(8)	0.442(1)	0.00175(1)	–3.15	–2.27(5)	0.72
RK251-43/44	OCc	0.371(3)	0.442(1)	0.00159(8)	–3.15	–2.27(5)	0.59	0.447(8)	0.446(4)	0.00148(1)	–3.10	–2.23(5)	0.59
RK252-43/44	OCd	0.371(3)	0.449(1)	0.00139(1)	–3.06	–2.20(5)	0.59	0.447(8)	0.447(1)	0.00139(1)	–3.08	–2.22(5)	0.55
RK253-43/44	OCe	0.371(3)	0.430(3)	0.00191(9)	–3.30	–2.40(4)	0.54	0.447(8)	0.429(2)	0.00192(14)	–3.31	–2.41(4)	0.53
$\log_{10}fO_2 = -9.67$, duration = 216 hr													
RK242-30	OCa	0.400(4)	0.355(1)	0.00143(3)e	–4.34	–3.31(1)	0.95						
RK243-21/30	OCb	0.400(4)	0.373(2)	0.00086(5)	–4.09	–3.08(2)	0.75	0.539(4)	0.374(2)	0.00085(3)	–4.07	–3.06(2)	0.76
RK244-21/30	OCc	0.400(4)	0.367(1)	0.00088(4)	–4.17	–3.15(2)	0.62	0.539(4)	0.365(3)	0.00094(2)	–4.20	–3.18(2)	0.63
RK245-21/30	OCd	0.400(4)	0.370(1)	0.0008(3)	–4.13	–3.12(2)	0.57	0.539(4)	0.367(2)	0.00085(1)	–4.17	–3.15(2)	0.57
RK246-21/21	OCe	0.400(4)	0.362(2)	0.00096(3)	–4.24	–3.21(1)	0.59	0.539(4)	0.359(1)	0.00095(1)	–4.28	–3.25(1)	0.51
$\log_{10}fO_2 = -9.22$, duration = 309.5 hr													
RK261-33	OCa							0.359(3)	0.322(1)	0.00109(2)	–4.82	–3.77(1)	0.98
RK262-14/33	OCb	0.314(3)	0.331(1)	0.00077(1)	–4.69	–3.64(1)	0.75	0.359(3)	0.330(1)	0.000784(3)	–4.70	–3.65(1)	0.75
RK263-14/33	OCc	0.314(3)	0.334(4)	0.00066(2)	–4.64	–3.60(1)	0.64	0.359(3)	0.334(1)	0.00067(2)	–4.65	–3.60(1)	0.63
RK264-14/33	OCd							0.359(4)	0.337(4)	0.00059(1)	–4.60	–3.56(1)	0.56
RK265-14/33	OCe							0.359(4)	0.326(2)	0.00074(5)	–4.76	–3.71(1)	0.55

[a] RKx-y/z: Experiment (x) with initial Pt-Fe alloy (y) in first pellet and (z) in second pellet; y and z refer to the run in Kessel et al. (2001) in which the inital alloy was produced.
[b] X_i^j = mole fractions of i in j based on three analyses for Cr and five for Fe in the Pt-alloys.
[c] γ_i^j = activity coefficients of i in j; model values calculated based on the Pt-Fe-Cr ternary model of Kessel et al. (2003).
[d] Activity of chromite in the spinel as calculated from Reaction 1b.
[e] Numbers enclosed in parentheses indicate one standard deviation of the distribution calculated by error propogation.

activity of chromite can be computed for an experiment from Equation 1b given the run conditions. We used ΔG_1^o and the Pt-Fe-Cr alloy activity model of Kessel et al. (2003) to calculate $a^{spinel}_{FeCr_2O_4}$ for each spinel composition in each of our experiments based on the known temperature, fO_2, and alloy composition. The chromite activities and activity coefficients for alloys obtained through the identity $\gamma_i^j = a_i^j / X_i^j$, where X_i^j is the mole fraction of component *i* in phase *j,* are given in Table 3. In Fig. 2, $a^{spinel}_{FeCr_2O_4}$ is shown as a function of $X^{spinel}_{FeCr_2O_4}$. Errors (1σ) on $a^{spinel}_{FeCr_2O_4}$ calculated using Equation 1b are 14–20% based on propagating the errors on temperature, fO_2, and alloy composition.

Also shown in Fig. 2 are activities calculated using MELTS (Ghiorso and Sack 1995) for spinel compositions examined in this study. The MELTS-calculated values at 1300 °C are directly comparable to our experiments and are in excellent agreement with our results. The values at 800 °C represent the corresponding activity-composition relationships according to MELTS at temperatures relevant to near-peak metamorphic temperatures of equilibrated ordinary chondrites (McSween and Patchen 1989; Kessel et al. 2002, Forthcoming). Wiser and Wood (1991), Von Seckendorff and O'Neill (1993), and O'Neill et al. (2003) among others have pointed out that the olivine model in MELTS may be considerably more non-ideal than it should be, and there continue to be improvements in thermodynamic data for end member phases such as chromite and picrochromite that are relevant to the present study (e.g., Klemme et al. 2000; Kessel et al. 2003) but are not yet incorporated into MELTS. Nevertheless, based on the results reported here and comparisons of predictions based on various models in the literature for olivine-spinel equilibria (e.g., Fabriès 1979; Engi 1983; Ballhaus et al. 1991; Sack and Ghiorso 1991a, b; Andersen et al. 1993) applied to experimental (e.g., Engi 1983; Thy et al. 1991) and natural (Fodor et al. 2002) systems, details of which are published elsewhere (Kessel et al. 2002, Forthcoming), we conclude that MELTS currently provides the best overall performance for spinel-based phase equilibria in equilibrated ordinary chondrites.

Oxygen Fugacity During Metamorphism of Ordinary Chondrites

In this section, we take two approaches to constraining conditions during metamorphism of ordinary chondrites. First, we use limits imposed by the coexistence of alloy,

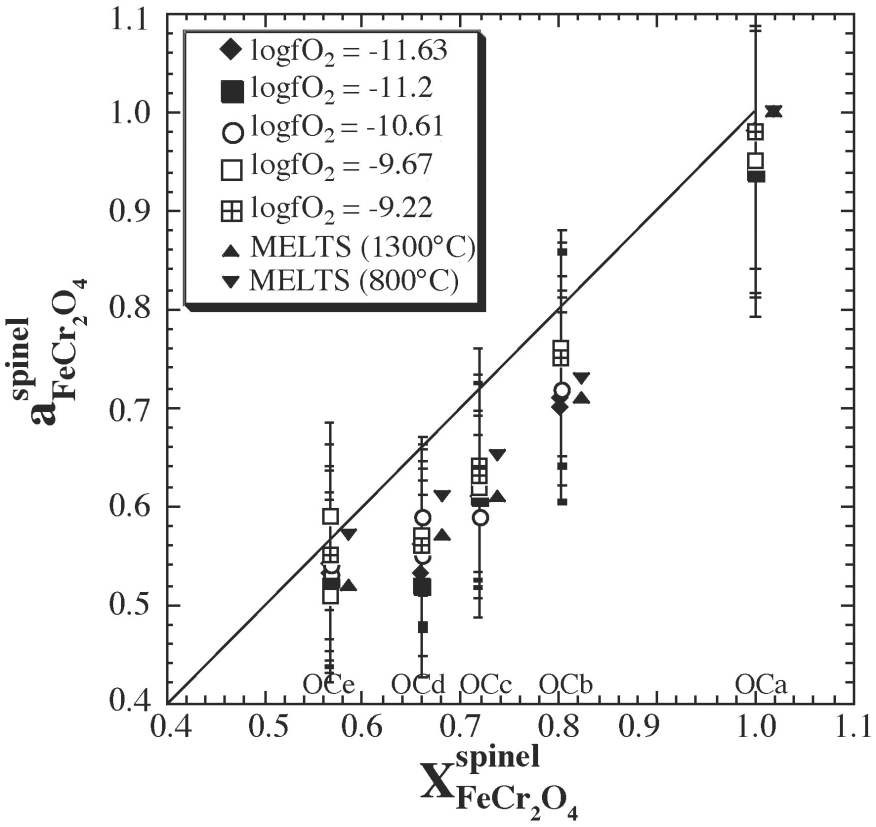

Fig. 2. Activity of chromite in spinels with compositions that represent equilibrated H chondrites as a function of $X^{spinel}_{FeCr_2O_4}$. Results of experiments from this study are represented by symbols with individual error bars (1σ). The solid thick line represents a 1:1 line, and the solid triangles represent activity-composition relationships calculated for our spinel compositions using the MELTS program (Ghiorso and Sack 1995) at 1300 °C and 800 °C displaced by 0.02 mole fractions of chromite for clarity.

orthopyroxene, and olivine to constrain possible values of temperature and fO_2. The proposed conditions for equilibrated ordinary chondrites must be consistent with these limits. Then, we calculate explicitly the T-fO_2 conditions experienced by equilibrated H chondrites during metamorphism based on the olivine + orthopyroxene + metal and spinel + metal phase assemblages.

Activities of components in the metal phase were calculated using the Fe-Ni-Cr model of Miettinen (1999). As discussed above, we assume a bulk value of 10 wt% Ni. Taenite is the stable phase in such a Fe-Ni alloy at temperatures above 728 °C. Below 728 °C, taenite precipitates kamacite, and the partitioning of elements between these two phases must be taken into account. For temperatures lower than 728 °C, we partitioned Ni between kamacite and taenite using the model of Miettinen (1999), which is consistent with the Fe-Ni phase diagram of Reuter et al. (1989). Note that, in an ideal binary Fe-Ni system, uncertainties in the bulk Ni content of the metallic phase have no effect on alloy compositions below the appearance temperature of kamacite because only kamacite/taenite ratios are affected, not their compositions. The effects of Cr and Co are negligible because of their low concentrations in the metal. The temperature at which kamacite begins to exsolve from the taenite is affected by the bulk Fe/Ni, but this effect is <10 °C if, as we have assumed, the bulk Ni content is in the range of 9.6–10.2 wt%. The use of a model for Fe-Ni-Cr ignores other minor components, most notably Co. The Co content of bulk metal in H chondrites is less than 0.5 wt% (Afiattalab and Wasson 1980). Since Raoult's law holds in the Fe-Co and Ni-Co binaries, the small amount of Co has little effect on the activity coefficients of Fe and Ni in the ternary (e.g., Fernández-Guillermet 1989), so our neglect of the effects of Co on the alloy thermochemistry does not introduce significant errors into calculations of fO_2.

We used the MELTS program (Ghiorso and Sack 1995) to calculate the activity of chromite in spinel at lower temperatures (<1000 °C; e.g., Dodd 1981; McSween and Patchen 1989; Kessel et al. 2002, Forthcoming) relevant to metamorphic conditions on the ordinary chondrite parent body. For consistency, activities of components in olivine and orthopyroxene were also calculated using MELTS based on measured mineral compositions. MELTS was also used to calculate the equilibrium constants for both reactions from the free energy of formation of the end members. Since free energies at elevated temperatures given by MELTS are relative to the elements at 298.15 K and 1 bar, it was first necessary to recalculate them relative to the stable elements at the temperature of interest and 1 bar. To be consistent with the reference state used by Miettinen (1999) for Fe-Ni-Cr alloys, we used Dinsdale's (1991) equations and a procedure similar to that described in Kessel et al. (2001) to revise the standard state of the elements for MELTS phases from 298.15 K to the temperature of interest.

The partitioning of Fe and Mg between olivine and spinel is temperature sensitive (e.g., Irvine 1965; Jackson 1969; Kessel et al. 2002, Forthcoming), and we used the thermodynamic model of Sack and Ghiorso (1991a, b) to express the equilibrium between these two phases by equating Fe-Mg exchange potentials. We chose the formulation of Sack and Ghiorso because based on comparison with experimental data, and when applied to natural systems, we conclude that it more accurately recovers these data than do other calibrations. Also, closure temperatures based on the MELTS calculation from olivine-spinel pairs are generally consistent with results based on other mineral assemblages (Kessel et al. 2002; Von Seckendorff and O'Neill 1993). For the three H4–6 chondrites included in this study, olivine-spinel equilibration temperatures vary little. Although there are subtle increases in minimum (677 → 741 °C), average (717 → 743 °C), and maximum (739 → 766 °C) temperatures with increasing petrographic type (Kessel et al. 2002, Forthcoming), they are small relative to the uncertainties in the olivine-spinel thermometer, and the temperature ranges overlap for all the H chondrites studied. Our results indicate peak temperatures for H4–6 chondrites of at least ~740 °C, regardless of petrographic type. The calculated olivine-spinel equilibration temperature in each meteorite allows us to constrain the corresponding fO_2.

Constraints Based on the Stability Limit of Orthopyroxene

Equilibrated ordinary chondrites are largely composed of olivine plus orthopyroxene with variable amounts of metal, sulfide, phosphate, feldspar, ilmenite, spinel, and clinopyroxene. If orthopyroxene in the presence of metal becomes too Fe-rich, it will break down, producing quartz and fayalitic olivine. Free silica is occasionally observed in equilibrated ordinary chondrites surrounded by a corona of Ca-poor and Ca-rich pyroxenes (e.g., Binns 1967; Olsen et al. 1981; Wlotzka and Fredriksson 1980; Brändstatter and Kurat 1985). These objects probably reflect the reaction of silica-rich glasses, which constitute ~1% of chondrules in highly unequilibrated ordinary chondrites (Brearley and Jones 1998), with olivine from the surrounding matrix to form pyroxenes (Olsen et al. 1981). This is clearly a non-equilibrium assemblage, as the pyroxene and silica are not in isotopic equilibrium (Olsen et al. 1981). Since there is no evidence for free silica in equilibrated ordinary chondrites that plausibly formed through the equilibrium decomposition of pyroxene (pyroxene is produced and silica consumed by corona formation), we conclude that the metamorphic conditions for equilibrated ordinary chondrites were on the reducing side of pyroxene breakdown to form silica and fayalitic olivine. In the following paragraphs, we consider the quantitative implications of this on T-fO_2 conditions for equilibrated ordinary chondrites.

Consider the stability of coexisting orthopyroxene, olivine, and metal. We assume that olivine composition is

well-described by the binary forsterite-fayalite and that orthopyroxene composition is well-described by enstatite-ferrosilite. The equilibrium:

$$Fe^{alloy} + FeSiO_3^{pyroxene} + \frac{1}{2}O_2 = Fe_2SiO_4^{olivine} \quad (2a)$$

is operative, from which an expression for fO_2 can be obtained:

$$fO_2 = \left(\frac{a_{FeSi_2O_4}^{olivine}}{\exp[-\Delta G_2^o / RT] a_{Fe}^{alloy} a_{FeSiO_3}^{pyroxene}} \right)^2 \quad (2b)$$

Equilibrium 2a can be combined with a corresponding equation for equilibrium Fe-Mg exchange between olivine and orthopyroxene:

$$Mg_2SiO_4^{olivine} + 2FeSiO_3^{pyroxene} = Fe_2SiO_4^{olivine} + 2MgSiO_3^{pyroxene} \quad (3)$$

Orthopyroxene compositions in equilibrium with olivine and metal in the Fe-Ni-Mg-Si-O system are shown for a set of isotherms in Fig. 3 for a bulk alloy containing 10 wt% Ni and neglecting Ni solubility in the silicates. Larimer (1968) experimentally studied the distribution of Fe between metal, olivine, and pyroxene as a function of fO_2 and temperature and gave a similar diagram for olivine compositions in the Ni-free case. From Fig. 3, the orthopyroxene becomes progressively more Fe-rich as the oxygen fugacity is increased at any given temperature. This cannot continue all the way to ferrosilite, however, because, for the low total pressures relevant to asteroidal sized bodies, Fe-rich orthopyroxenes break down to form olivine plus quartz. We calculated the composition of the pyroxene at 1 bar for which this occurs through the equilibrium constant for the reaction:

$$2FeSiO_3^{pyroxene} = SiO_2^{quartz} + Fe_2SiO_4^{olivine}$$

and display the results in Fig. 3 by truncating isotherms at the limiting oxygen fugacities and Fe content in orthopyroxene above which the orthopyroxene is unstable. Superimposed on the 1100 and 1200 °C isotherms are experimental results by Larimer (1968) and Nafziger and Muan (1967) showing good agreement with our calculations. The range of orthopyroxene compositions found in equilibrated ordinary chondrites

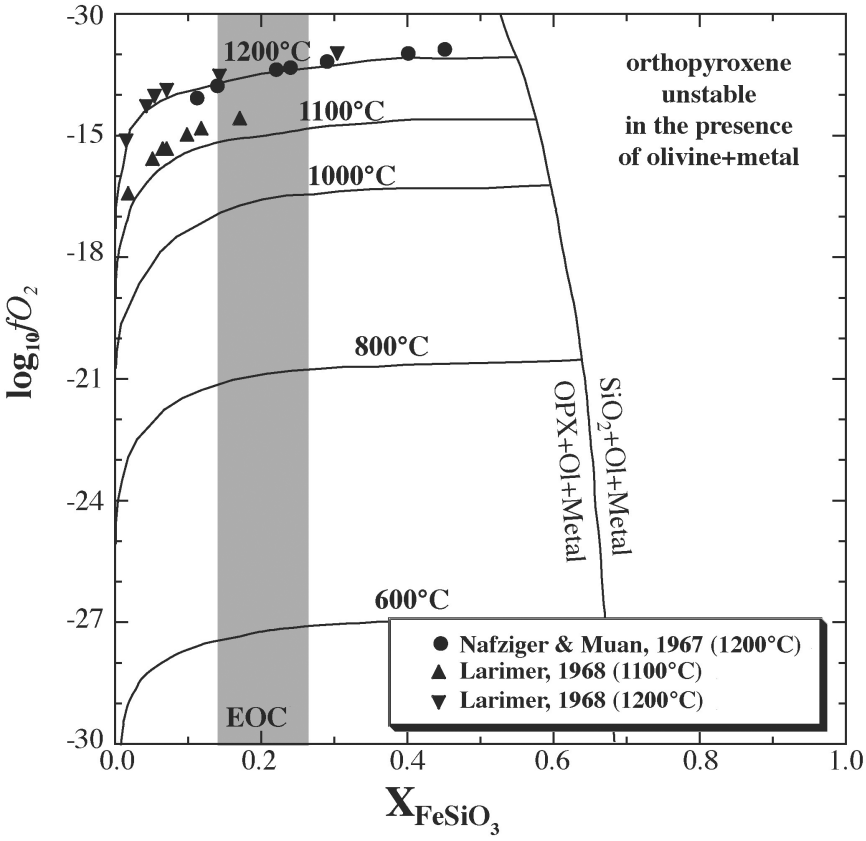

Fig. 3. Orthopyroxene (OPX) composition in equilibrium with olivine (Ol) and metal with 10 wt% Ni as a function of $\log_{10}fO_2$ at a total pressure of 1 bar and temperature calculated using the program MELTS (Ghiorso and Sack 1995). The isotherms are truncated by the pyroxene breakdown curve indicating the limiting $\log_{10}fO_2$ for the most Fe-rich stable orthopyroxene. Experimental results at 1100 and 1200 °C from Nafziger and Muan (1967) and Larimer (1968) are also shown. The shaded region represents the range of orthopyroxene compositions found in equilibrated ordinary chondrites (EOC) taken from Brearley and Jones (1998). See text for further explanation.

(Brearley and Jones 1998) is also shown for reference. Proposed metamorphic conditions for equilibrated ordinary chondrites that are more oxidizing than the orthopyroxene stability limit are inconsistent with the observed phase assemblage.

Olivine + Orthopyroxene + Metal Oxygen Barometer

Reaction 2a is the basis for several classic studies of T-fO_2 conditions in ordinary chondrites (e.g., Mueller 1964; Larimer 1968; Williams 1971b; McSween and Labotka 1993). To determine oxygen fugacity based on this equilibrium, we used activities of components in the solid phases calculated from the models of Ghiorso and Sack (1995) and Miettinen (1999) for each analyzed olivine + orthopyroxene + metal assemblage. The $\log_{10}fO_2$ at a given temperature was calculated for the equilibrium taenite (either the single high temperature phase or taenite in equilibrium with kamacite at lower temperatures at which two metal phases are stable) consistent with a bulk alloy containing 10 wt% Ni and our measured olivine and orthopyroxene compositions. Note that calculated values using kamacite instead of taenite at the lower temperature conditions at which both metal phases are present are identical as required for internal consistency of the thermodynamic data. The calculated $\log_{10}fO_2$s for olivine + orthopyroxene + metal computed at the olivine-spinel equilibration temperatures are shown in Fig. 4a for each assemblage in each meteorite. The average $\log_{10}fO_2$ based on all assemblages in all meteorites is IW – 2.51 ± 0.05 (1σ), and all individual results lie in the range of 2.44–2.62 log units below IW.

At equilibrium at a given temperature, Reaction 3 indicates that olivine and orthopyroxene compositions co-vary as a function of oxygen fugacity. To check the degree to which olivine and orthopyroxene reached equilibrium, we calculated the orthopyroxene composition in equilibrium with the determined olivine composition at the olivine-spinel equilibration temperatures for each assemblage in each meteorite and used this composition to obtain fO_2 through Reaction 2a. The $\log_{10}fO_2$s based on assuming olivine and orthopyroxene are in equilibrium are 0.2–0.3 log units more oxidizing than values computed based on both mineral compositions, indicating that both phases are close to equilibrium.

Note that the inferred fO_2 values are so low that they cannot actually be thought of in terms of a concentration of O_2 molecules in a coexisting gas phase; under these circumstances, the calculated fO_2 values may be more appropriately thought of as a proxy for H_2/H_2O because Reaction 2a can be combined with the water oxidation reaction $H_2O + H_2 = 1/2O_2$ to give:

$$Fe^{alloy} + FeSiO_3^{pyroxene} + H_2O = Fe_2SiO_4^{olivine} + H_2$$

Assuming that the partial pressure of H_2 during metamorphism of ordinary chondrites was close to the total vapor pressure, the inferred oxygen fugacities indicate that the partial pressure of H_2O was roughly 1–3% of the total pressure.

The small range in fO_2 around the average may reflect the small temperature range of olivine-spinel equilibration temperatures for our suite (677–766 °C). How would these results change if closure temperatures for olivine-spinel equilibrium and olivine-pyroxene-alloy equilibrium differed significantly? There is a correlation between calculated olivine-spinel temperatures and spinel grain size (Kessel et al. 2002, Forthcoming), with smaller grains generally recording lower temperatures; this suggests that the olivine-spinel thermometer records retrograde conditions. Closure temperatures for olivine-pyroxene-alloy assemblages are not known, but they are almost certainly higher than for olivine-spinel assemblages because diffusion of Fe/Mg in orthopyroxene is slower than in olivine or spinel (Ozawa 1984; Ganguly and Tazzoli 1994; Ganguly et al. 1994) and because spinels are much smaller than coexisting olivine grains in equilibrated ordinary chondrites (i.e., reequilibration of spinel cores should occur to lower temperatures than for cores of coexisting olivine or pyroxene grains). Note that although diffusion can take place in the alloys to much lower temperatures than in the silicates or spinel (Ozawa 1984; Jönsson 1995), this would not have much of an effect on calculated fO_2 because the Fe/Ni ratio, which dictates the Fe activity, does not change significantly as a function of temperature. Therefore, olivine-spinel temperatures based on core compositions of phases are plausibly lower boundaries on closure temperatures for the olivine-pyroxene-alloy oxygen barometer.

An upper limit on temperature can be obtained from two-pyroxene thermometry, which is thought to approximate peak metamorphic conditions (Dodd 1981). Based on two-pyroxene thermometry using the high Ca-limb of the solvus and the model of Lindsley (1983), Olsen and Bunch (1984) determined metamorphic temperatures for five type H6 chondrites in the range of 800–850 °C. Harvey et al. (1993) used the same thermometer for six H6 chondrites and obtained generally higher temperatures: 898 ± 86 °C for three Antarctic and 932 ± 50 °C for three non-Antarctic samples. Estimates from both studies exceed those recorded by olivine-spinel equilibration. The eutectic melting temperature for alloy + troilite in the system Fe-Ni-S (~990 °C; Chuang et al. 1985; Hsieh et al. 1987) provides another upper limit on peak temperature as there is no textural evidence for this assemblage having melted during metamorphism (e.g., Dodd 1981), and chondrite bulk compositions have no evidence of chalcophile element depletions consistent with mobilization of a sulfide-rich melt (e.g., Jarosewich 1990). Taking the maximum olivine-spinel temperature for each meteorite and 990 °C as extreme limits for the possible closure temperature for olivine-orthopyroxene-alloy assemblages, we calculate that oxygen fugacities for H4–6 chondrites were in the range IW – 2.56 to

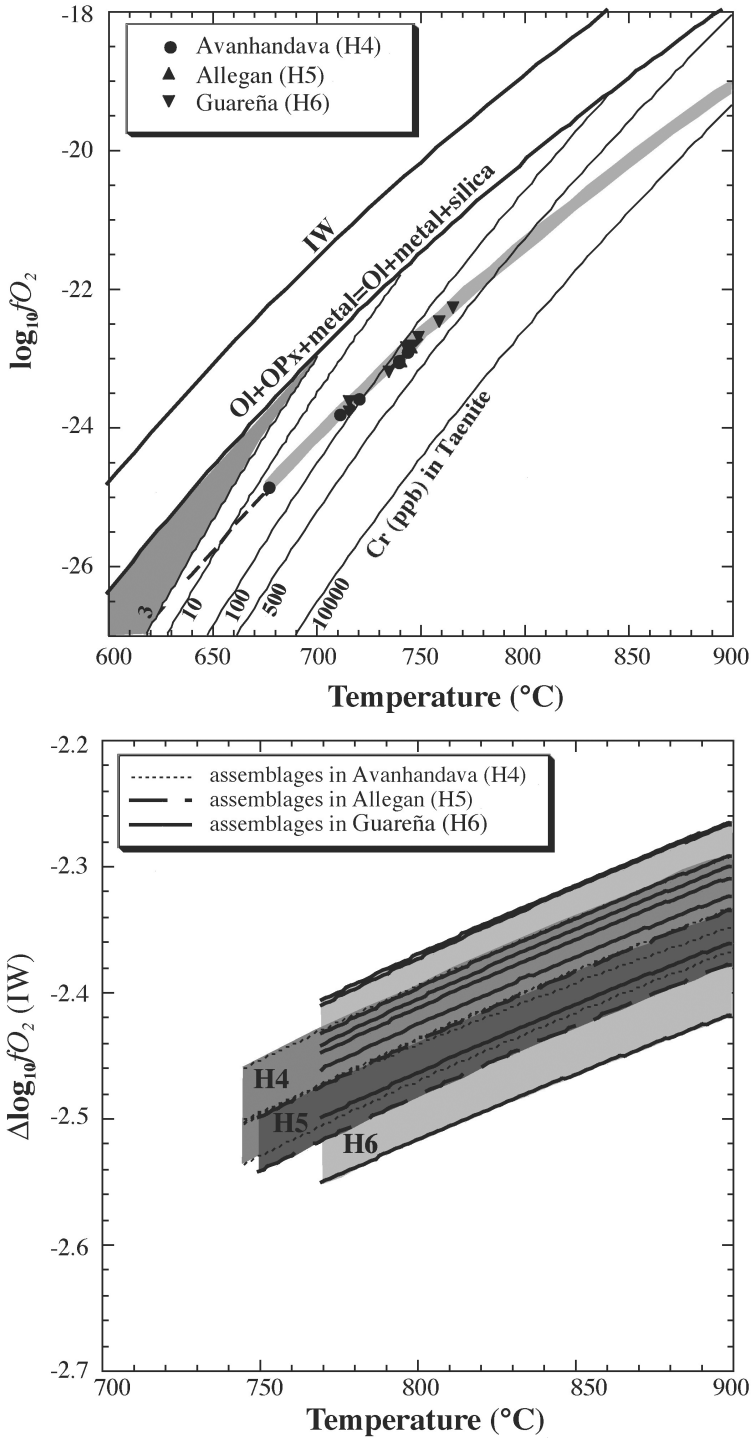

Fig. 4. Values of $\log_{10}fO_2$ as a function of temperature: a) general constraints. The symbols refer to conditions based on individual olivine + pyroxene + metal assemblages. The dashed curve was determined from an unweighted regression of calculated $\log_{10}fO_2$ for these data as a function of temperature. The light shaded zone represents $\log_{10}fO_2$ values constrained by the olivine + pyroxene + metal assemblages at temperatures above spinel-metal equilibration. The thin solid curves show T-fO_2 conditions for spinel in equilibrium with taenite with a Cr concentration (ppb wt) that is specified adjacent to the curve. Temperature-$\log_{10}fO_2$ values inside the shaded region are consistent with chromite in equilibrium with taenite containing ≤3 ppb Cr. Thick solid curves denoting the iron-wüstite (IW) buffer and the pyroxene breakdown curves are also shown; b) detail of calculated curves for individual olivine-pyroxene-alloy assemblages. Each curve represents the $\log_{10}fO_2$ determined based on calculated activities of components in the solid phases for analyzed phase compositions at each temperature. The shaded regions are bands encompassing T-$\log_{10}fO_2$ for assemblages in a given meteorite. For each meteorite, curves are truncated at the maximum olivine-spinel temperature, and the shading envelopes possible T-fO_2 conditions experienced by each meteorite.

IW – 2.19. For the "reasonable" maximum temperature of 900 °C, the range would be IW – 2.56 to IW – 2.27. Based on Fig. 4b, there is no trend of increasing or decreasing fO_2 relative to IW as a function of metamorphic type as the entire range of conditions is encompassed by Guareña assemblages and the average for each metamorphic type referenced to a constant temperature (e.g., IW – 2.33 for H4, IW – 2.36 for H5, and IW – 2.32 for H6 at 900 °C) does not vary systematically with type.

Our calculations ignore the effect of total pressure (i.e., all are referenced to 1 bar), but we can assess the influence of this parameter on our results. Asteroids of the order of ~50–100 km diameter are thought to be the parent bodies from which ordinary chondrites were derived (Rubin et al. 1988; Wetherill and Chapman 1988). The maximum pressure in such a body with a density of 3.41 g/cm^3 (the average density of H4–6 falls; Wilkison and Robinson 2000) is therefore 10–40 bars. For olivine + orthopyroxene + metal assemblages with constant phase compositions at the calculated olivine-spinel equilibration temperature, we recalculated component activities and equilibrium constants (Reaction 2a) at a pressure of 40 bars. These calculations lead to oxygen fugacities 0.007 log units more oxidizing at the center of 100 km diameter parent body than they would be at the surface. Differences at this level are not significant for deciphering the gross features of the T-$\log_{10}fO_2$ relationships of the ordinary chondrites.

Spinel + Metal Oxygen Barometer

The second equilibrium we examined as a constraint on fO_2 involves the coexistence of spinel and metal as described by Reaction 1a. In our experiments, temperature and fO_2 were known, and the equilibrium was used to constrain alloy (Kessel et al. 2001) or chromite (see above and Kessel et al. [2003]) activities. For application to the ordinary chondrites, activities are calculated as a function of temperature for the coexisting spinel and metal, and we can then calculate the fO_2 for each meteoritic phase assemblage given a temperature. Since spinels in the meteorites studied in this work are similar in composition to the synthesized OCd spinel used in our experiments, we calculated chromite activities in OCd spinel using MELTS. Only limiting values of the oxygen fugacity experienced by equilibrated ordinary chondrites can be obtained from Reaction 1a, however, because only an upper limit on the concentration of Cr is available (3 ppb). Taenite provides the most restrictive constraints on fO_2 for a given Cr content. Chromium preferentially partitions into taenite relative to kamacite according to the thermodynamic model of Miettinen (1999) and as confirmed by observed Cr distributions in taenite-kamacite in unequilibrated ordinary chondrites (e.g., Rambaldi et al. 1984). Thus, for the same olivine and pyroxene compositions and bulk Fe/Ni in the metallic phase, Reaction 1a leads to a higher limiting fO_2 for taenite than it does for kamacite with the same Cr content. For Allegan and Guareña, calculations using 3 ppb Cr in taenite are applicable; for Avahandava, the corresponding lower limits for this meteorite are more reducing by 0.7 log units for temperatures between 600–800 °C because we analyzed only kamacite.

Temperature-fO_2 conditions consistent with observed spinel compositions in equilibrated H chondrites and the limit of 3 ppb Cr in taenite are restricted to the darker shaded region shown in Fig. 4a or its extension to lower temperatures. If the temperatures determined from olivine-spinel thermometry were appropriate for spinel + metal equilibria, then fO_2s exceeding those of the pyroxene breakdown reaction would be required to explain the undetectable Cr contents of the metal (Fig. 4a). Even if such oxidizing conditions were accepted, the corresponding compositions of olivine and pyroxene would bear no resemblance to those observed in equilibrated ordinary chondrites (see, e.g., Fig. 3). This suggests that closure temperatures for spinel + metal were, in fact, lower than (and perhaps much lower than) 700 °C; this is consistent with faster Cr diffusion in Fe-Ni-Cr alloys compared to Fe/Mg in olivine and spinel ($\log_{10}D_{Cr}$ [700 °C] in Fe-Ni-Fe metal is ~–15 [Jönsson 1995]; $\log_{10}D_{Fe/Mg}$ [700 °C] in olivine and spinel is ~–19 [Ozawa 1984]). Assuming that oxygen fugacities relevant to spinel + metal equilibration were restricted to the dashed curve in Fig. 4a, then closure temperatures for spinel + metal in Allegan and Guareña were below ~625 °C. For Avahandava, we only determined limiting Cr concentrations in kamacite, so the limiting temperature based on spinel + metal is a little higher (~660 °C).

Our conclusion that closure temperatures for alloy-spinel equilibration were considerably lower than olivine-spinel rests on the position of the 3 ppb isopleth in Fig. 4a. For alloy-spinel temperatures to be the same as those determined from olivine-spinel thermometry, the 3 ppb Cr isopleth in Fig. 4a would need to pass through the high temperature end of the olivine-spinel data. Such a shift would require an 80 kJ/mole adjustment to the free energy of Reaction 1a with corresponding errors in one or more of the variables in Equation 1b. Here, we provide a brief discussion of the possible errors. Values of ΔG_1^o are known to within a few kJ, and replacing the values computed through MELTS with updated expressions of Klemme et al. (2000) and Kessel et al. (2003) actually lowers the intersection of the 3 ppb isopleth and the curve for olivine-spinel by 10 degrees. The well-constrained activities of iron in the alloys (Miettinen 1999) allow only trivial shifts in the calculated isopleths. Metallic Cr is a little more problematic. For atomic Fe/Ni = 9.5, the value of meteoritic interest, Cr is Henrian at concentrations below 15000 ppb in the temperature range 600–800 °C, according to the model of Miettinen (1999). It is possible that a different substitution mechanism pertains to extremely low Cr concentrations and that the Henry's law coefficient determined by Miettinen (1999) does not apply (the correct activity coefficient would need to be ~50 times higher). As far as we are aware, however, no such effect has been demonstrated for Fe-Ni-Cr or any other ferrous alloy.

Chromite activities are an unlikely source for shifting the isopleths to higher temperatures. For our highest olivine-spinel equilibration temperature, a chromite activity of 0.00002 would be required to make the 3 ppb isopleth match the same T-$\log_{10}fO_2$, far lower than experimentally determined values at higher temperatures (~0.56 at 1300°C for data from this study). Such low activities for such Cr-rich chromites are inconsistent with existing chromite-bearing binary spinel phase diagrams and low temperature galvanic cell measurements. For example, Jacob and Iyengar (1999) measured chromite activities in the binary chromite-pichrochromite and showed that the phase behaves as a regular solution in the temperature range 777–1077 °C. This means that activities of chromite in Cr-rich spinels at constant composition are a very weak function of temperature, changing by just 1 or 2% between 1300°C and 600°C, far less than needed to account for a significant shift in the position of the 3 ppb isopleth. Finally, the effects of pressure on spinel + metal equilibria are also small. For identical phase compositions at the same temperature, oxygen fugacities based on olivine-spinel equilibria would be 0.012 log units more oxidizing at the center of a 100 km-diameter parent body than they would be at 1 bar, essentially the same effect calculated above for olivine + orthopyroxene + metal. Thus, we infer that the most plausible explanation for the undetectable Cr contents of alloys in equilibrated chondrites is that the closure temperatures of spinel + metal equilbria were at least 50–150 °C lower than those of spinel + olivine equilibria.

Comparison with Previous Work

Two approaches have been used to determine oxygen fugacities for equilibrated ordinary chondrites. The first and most widely used approach combines the compositions of coexisting phases with thermochemical data to constrain *f*O2 (e.g., Mueller 1964; Larimer 1968; Williams 1971b; McSween and Labotka 1993); this is the approach used in this study. The second approach, used by Walter and Doan (1969) and Brett and Sato (1984), is based on measurements of "intrinsic" oxygen fugacities using a solid-electrolyte, double-cell technique. In this section, we compare our results with those in the literature based on these two approaches. Figure 5 compares literature values to our constraints on $\log_{10}fO_2$ based on olivine + orthopyroxene + metal and spinel + metal equilibria.

Oxygen Barometry

Using Reaction 2a, Mueller (1964) assumed that olivine and orthopyroxene coexisting with metallic iron are ideal solutions and calculated T-$\log_{10}fO_2$ curves as functions of olivine composition. Larimer (1968) experimentally determined compositions of olivine and pyroxene in equilibrium with Fe metal as a function of temperature and fO_2 and applied regular solution models to both olivine and pyroxene. Both Mueller (1964) and Larimer (1968) treated the alloy as pure Fe, and neither presented specific calculations for observed mineral compositions in meteorites. Larimer did not suggest specific T-fO_2 conditions for ordinary chondrites, but based on the range of silicate compositions given in Ringwood (1961), Mueller (1964) suggested a $\log_{10}fO_2$ of IW – 2.03 ± 0.5 at 827 °C. This result is slightly more oxidizing than our estimates based on the same reaction, which are IW – 2.34 to IW – 2.49 at 827 °C, as shown in Fig. 5. The difference reflects Mueller's (1964) assumption of a pure Fe metallic phase, his use of ideal activity-composition models for all solid phases, and the improvements in thermochemical data on end member phases since the publication of his work. Using Reactions 2a and 3, Williams (1971b) calculated temperatures of 880 ± 150 °C and pressures of 5 ± 5 kbar for ordinary chondrites of all groups based on compositions of coexisting olivine and pyroxene in types 5 and 6 equilibrated ordinary chondrites from Ringwood (1961), Keil and Fredriksson (1964), and Van Schmus (1969) and assuming ideal solutions for olivine and pyroxene. Based on the observed metal composition in ordinary chondrites, Williams (1971b) assumed a Fe activity of 0.5 and obtained $\log_{10}fO_2$ of IW – 0.47 ± 1.2 at 880 °C, about 2 log units more oxidizing than obtained in this study. Most of the discrepancy with our results is driven by differences in the equilibrium constants used for Reaction 2a. We used values calculated by MELTS, which relate back to the compilation of Berman (1988) and are in agreement with values derived by Holland and Powell (1990) and Guddmundsson and Holloway (1993), while Williams (1971b) used considerably different values given by Williams (1971a). Williams' (1971a) equilibrium constant contributes 1.20 log units of the difference between his calculated fO_2 and ours. The differences in activity models for olivine and pyroxene contribute –0.6 log units of the difference, and assuming Fe activity of 0.5 instead of ~0.9 increases the fO_2 by 0.5 log units. The $\log_{10}fO_2$ obtained by Williams (1971b) is more oxidizing than the pyroxene breakdown curve calculated using MELTS but is on the pyroxene breakdown curve calculated using Williams' (1971a, b) data.

McSween and Labotka (1993) used an approach similar to ours for exploring the implications of coexisting olivine, pyroxene, and metal for the T-fO_2 conditions of equilibrated ordinary chondrites. The differences between their approach and ours are that they used Reaction 2a to calculate oxygen fugacities constrained by the mineral compositions relative to the fayalite-iron-ferrosilite (FIF) buffer and followed Mueller (1964) in treating olivine and pyroxene as ideal solutions and assuming the metallic phase to be pure Fe. Given this set of assumptions, all activities of the solid phases are independent of temperature, and deviations of fO_2 from the metastable FIF buffer are functions only of the olivine and pyroxene compositions, i.e., temperature does not affect the relative fO_2 values. McSween and Labotka (1993) assumed metamorphic

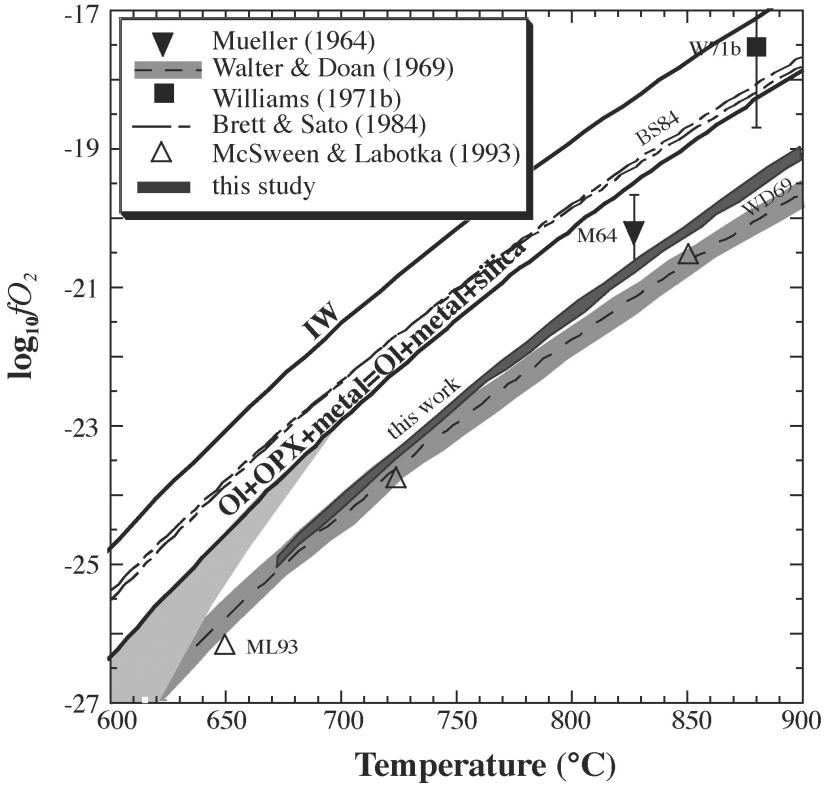

Fig. 5. Summary of $\log_{10}fO_2$ estimates as a function of temperature for equilibrated H chondrites based on this and previous studies. $\log_{10}fO_2$ values from this study are represented by a dark shaded region for olivine + pyroxene + metal assemblages and a more lightly shaded region for spinel + metal. Limiting curves based on the stability of alloy and pyroxene are also shown. Oxygen fugacities more oxidizing than either of these curves are inconsistent with the observed phases of equilibrated ordinary chondrites. Literature data are from Mueller (1964; M64); Walter and Doan (1969; WD69) (shaded area indicates ±0.1 log units uncertainty); Williams (1971b; W71b); Brett and Sato (1984; BS84); and McSween and Labotka (1993; ML93).

temperatures for equilibrated ordinary chondrites from Dodd (1981) and translated increases in Fe/(Fe + Mg) of olivine and pyroxene with petrographic type (see discussion below) into a corresponding increase in $\log_{10}fO_2$ from –26.16 at 650°C (IW – 3.24) for type 4 to –23.77 at 725 °C (IW – 3.07) for type 5 to –20.51 at 850 °C (IW – 2.85) for type H6 chondrites. As shown in Fig. 5, these values are similar to more reducing than those determined in this study (i.e., IW – 2.32 to IW – 2.47 referenced to 850°C) for the same equilibrium, reflecting the different activity models (contributing ~0.2 log units of the difference) and metal composition (contributing ~0.15 log units).

Intrinsic fO_2 Measurements

Walter and Doan (1969) and Brett and Sato (1984) measured intrinsic oxygen fugacities in equilibrated ordinary chondrites using a solid-electrolyte, double-cell method. The EMF was determined during cycles of heating and cooling; these measurements yielded a T-$\log_{10}fO_2$ relationship for each meteorite that was then assumed to be equivalent to conditions during metamorphism. Walter and Doan (1969) reported $\log_{10}fO_2$ values ranging from IW – 2.81 (600 °C) to IW – 3.01 (900 °C) in Guareña (H6) with a stated uncertainty on individual measurements of approximately ±0.1 log units. This result is in fair agreement with our values for the same meteorite (e.g., IW – 2.27 to IW – 2.42 referenced to 900 °C). In a more extensive study, Brett and Sato (1984) measured intrinsic oxygen fugacities in several ordinary chondrites including two H chondrites, Ochansk (type 4) and Guareña (type 6). The measured $\log_{10}fO_2$ for Ochansk ranges from IW – 0.71 (600 °C) to IW – 0.93 (900 °C) and for Guareña from IW – 1.07 (600 °C) to IW – 1.12 (900 °C) (Fig. 5). These conditions are much more oxidizing than either the intrinsic fO_2 measurements of Walter and Doan (1969) for Guareña or the oxygen barometry results of McSween and Labotka (1993) and this study. Moreover, as shown in Fig. 5, Brett and Sato's (1984) oxygen fugacities plot above the pyroxene breakdown curve and are, therefore, inconsistent with the observed phase assemblages of ordinary chondrites.

A problem with intrinsic fO_2 measurements is that the phase equilibria that control the observed EMFs may have little if anything to do with formation conditions of the rock/mineral being examined (e.g., Virgo et al. 1988). For example, oxygen released from altered minerals (e.g., rusty metal grains) can dominate the recorded signal and result in higher than primary fO_2 values. Alternatively, oxidation of graphite or organic

materials during heating can consume available oxygen and lead to more reducing values; there is evidence that EMFs from single mineral measurements are generally dominated by organic contaminants (e.g., Mattioli and Wood 1986; Virgo et al. 1988). However, Brett and Sato (1984) were aware of these potential difficulties and examined rocks containing a multi-phase assemblage that, in principle, should have been capable of buffering the local environment in the cell; moreover, they studied only falls and removed visibly rusted grains. Nevertheless, their measured EMFs may reflect the incorporation of oxidized regions in the rocks or contamination of the cell, as evidenced by the fact that their fO_2 results for Semarkona (LL3), Cherokee Springs (LL5), and Guareña (H6) became more oxidizing with time as heating/cooling cycles were repeated. Given the vulnerability of intrinsic oxygen fugacity measurements of metal-bearing meteorites to auto-oxidation, the unexplained disagreement between the intrinsic fO_2 measurements of Walter and Doan (1969) and Brett and Sato (1984) for Guareña, and the implication of oxygen fugacities more oxidizing than the pyroxene stability limit, we agree with the conclusion of McSween and Labotka (1993) that the oxygen fugacities obtained by Brett and Sato (1984) are too oxidizing to be plausible.

Oxidation with Progressive Metamorphism?

Our calculated oxygen fugacities based on olivine-orthopyroxene-metal assemblages in type 4–6 equilibrated H chondrites are 2.19–2.56 log units below IW during near-peak metamorphism (740–990 °C) with no evidence for major shifts in fO_2 that correlate with the degree of metamorphism. McSween and Labotka (1993) summarized a number of observations, such as decreases in bulk metal content and increases in mean FeO concentrations in olivine and pyroxene and Ni/Fe as a function of increasing metamorphic type. Although the errors on mean values for each metamorphic type exceed the changes being considered in almost every instance, the changes appear systematic, and they attributed these variations to progressive oxidation accompanying metamorphism. McSween and Labotka (1993) calculated oxygen fugacities relative to the FIF buffer based on olivine-pyroxene-alloy equilibria and obtained a temperature-independent increase of 0.03 log units between H4 and H6 chondrites. Our calculations using the average phase compositions of McSween and Labotka (1993) with the MELTS model for the solid solutions suggest that, referenced to any specific temperature between 600 and 990 °C, the average fO_2 of an H6 chondrite must be 0.01–0.02 log units higher than that of an H4. Although very small, this is not likely to result from differences in total pressure between the H4 and H6 chondrites, i.e., this difference could only be accounted for in a system of constant bulk composition if the equilibrium pressures of H6 meteorites were 150–280 bars higher than those of H4 meteorites, and this would require a parent body with a radius >160 km. Variations in equilibration temperature for a system of constant total composition might, however, help to explain a range of oxidation states because, for constant compositions of olivine, pyroxene, and metal, the fO_2 relative to FIF or IW becomes more oxidizing with increasing temperature. For example, equating the peak metamorphic temperatures of McSween et al. (1988) of H4 (600–700 °C) → H5 (700–750 °C) → H6 (750–950 °C) with equilibration temperatures for olivine-pyroxene-alloy oxygen barometry implies that H6 chondrites were 0.2–0.3 log units more oxidizing relative to FIF than H4s. If, as suggested by Kessel et al. (2002, Forthcoming), all H chondrites experienced peak metamorphic temperatures of at least 740 °C (i.e., the range is not more than 740–950 °C), the corresponding difference is <0.2 log units. McSween and Labotka (1993) could not quantify these effects because their thermodynamic model required T-fO_2 curves parallel to FIF. Thus, we can not dismiss an increase (or decrease) in oxygen fugacity with increasing petrographic type, but our results restrict such effects to no more than 0.2 log units, on average, in terms of fO_2.

CONCLUSIONS

Knowledge of the oxygen fugacities experienced by ordinary chondrites is important for understanding the metamorphic conditions prevailing on their parent bodies. Based on equilibrium of olivine, pyroxene, and alloy in equilibrated H chondrites, all experienced similar fO_2s, 2.19–2.56 log units below IW assuming equilibration temperatures in the range of 740–990 °C, regardless of petrographic type or metamorphic temperature. T-fO_2 conditions calculated based on the detection limit for Cr in alloys (3 ppb) are consistent with those for olivine + orthopyroxene + metal if closure temperatures for spinel + metal exchange were below ~625 °C for Allegan and Guareña and below ~660 °C for Avanhandava.

Acknowledgments–This work was supported by NASA grants NAG-10423 and NNG04GG14G. Discussions with Mike Baker and Hap McSween inspired parts of this work and led to significant improvements in the quality of this study. Ma Chi and Yunbin Guan are thanked for their help with the analytical work. The authors thank A. A. Ariskin, M. S. Ghiorso, H. St. C. O'Neill and K. Righter for their reviews. Thin sections were generously provided by the Smithsonian Institution. Division contribution # 5715.

Editorial Handling—Dr. Kevin Righter

REFERENCES

Afiattalab F. and Wasson J. T. 1980. Composition of the metal phases in ordinary chondrites: Implications regarding classification and metamorphism. *Geochimica et Cosmochimica Acta* 44:431–446.

Andersen D. J., Lindsley D. H., and Davidson P. M. 1993. QUILF—A Pascal program to assess equilibria among Fe-Mg-Mn-Ti oxides, pyroxenes, olivine, and quartz. *Computers and Geosciences* 19:1333–1350.

Ballhaus C., Berry R. F., and Green D. H. 1991. High pressure experimental calibration of the olivine-orthopyroxene-spinel oxygen geobarometer: Implications for the oxidation state of the upper mantle. *Contributions to Mineralogy and Petrology* 107: 27–40.

Bennett M. E. and McSween H. Y. 1996. Revised model calculations for the thermal histories of ordinary chondrite parent bodies. *Meteoritics & Planetary Science* 31:783–792.

Berman R. G. 1988. Internally-consistent thermodynamic data for minerals in the system Na_2O-K_2O-CaO-MgO-FeO-Fe_2O_3-Al_2O_3-SiO_2-TiO_2-H_2O-CO_2. *Journal of Petrology* 29:445–522.

Binns R. A. 1967. Farmington meteorite: Cristobalite xenoliths and blackening. *Science* 156:1222–1226.

Bischoff A. and Keil K. 1983. Ca-Al-rich chondrules and inclusions in ordinary chondrites. *Nature* 303:588–592.

Bischoff A., Palme H., and Spettel B. 1989. Al-rich chondrules from the Ybbsitz-H4 chondrite: Evidence for formation by collision and splashing. *Earth and Planetary Science Letters* 93:170–180.

Brändstatter F. and Kurat G. 1985. On the occurrence of silica in ordinary chondrites (abstract). *Meteoritics* 20:615–616.

Brearley A. J. and Jones R. H. 1998. Chondritic meteorites. In *Planetary materials,* edited by Papike J. J. Washington D. C.: Mineralogical Society of America. pp. 3-1–3-398.

Brett R. and Sato M. 1984. Intrinsic oxygen fugacity measurements on seven chondrites, a pallasite, and a tektite and the redox state of meteorite parent bodies. *Geochimica et Cosmochimica Acta* 48:111–120.

Bunch T. E., Keil K., and Snetsinger K. G. 1967. Chromite composition in relation to chemistry and texture of ordinary chondrites. *Geochimica et Cosmochimica Acta* 31:1569–1582.

Buseck P. R. and Keil K. 1966. Meteoritic rutile. *American Mineralogist* 51:1506–1515.

Chamberlin L., Beckett J. R., and Stolper E. 1994. Pd-oxide equilibration: A new experimental method for the direct determination of oxide activities in melts and minerals. *Contributions to Mineralogy and Petrology* 116:169–181.

Chuang Y. -Y., Hsieh K. -C., and Chang Y. A. 1985. Thermodynamics and phase relationships of transition metal-sulfur systems. Part V. A reevaluation of the Fe-S system using associated solution model for the liquid phase. *Metallurgical Transactions* 16B:277–285.

Dinsdale A. T. 1991. SGTE data for pure elements. *Calphad* 15:317–425.

Dodd R. T. 1969. Metamorphism of the ordinary chondrites: A review. *Geochimica et Cosmochimica Acta* 33:161–203.

Dodd R. T. 1981. *Meteorites, a petrologic-chemical synthesis.* New York: Cambridge University Press. 368 p.

Engi M. 1983. Equilibria involving Al-Cr spinel: Mg-Fe exchange with olivine. Experiments, thermodynamic analysis, and consequences for geothermometry. *American Journal of Science* 283A:29–71.

Fabriès J. 1979. Spinel-olivine geothermometry in peridotites from ultramafic complexes. *Contributions to Mineralogy and Petrology* 69:329–336.

Fernández-Guillermet A. 1989. Assessing the thermodynamics of the Fe-Co-Ni system using a CALPHAD predictive technique. *Calphad* 13:1–22.

Fodor R. V., Sial A. N., and Gandhok G. 2002. Petrology of spinel peridotite xenoliths from northeastern Brazil: Lithosphere with a high geothermal gradient imparted by Fernando de Noronha plume. *Journal of South American Earth Sciences* 15:199–214.

Fredriksson K., Nelen J., and Fredriksson B. J. 1968. The LL-group chondrites. In *Origin and distribution of the elements,* edited by Ahrens L. H. New York: Pergamon Press. pp. 457–466.

Ganguly J. and Tazzoli V. 1994. Fe^{2+}-Mg interdiffusion in orthopyroxene: Retrieval from the data on intracrystalline exchange reaction. *American Mineralogist* 79:930–937.

Ganguly J., Yang H., and Ghose S. 1994. Thermal history of mesosiderites: Quantitative constraints from compositional zoning and Fe-Mg ordering in orthopyroxenes. *Geochimica et Cosmochimica Acta* 58:2711–2723.

Gastineau-Lyons H. K., McSween H. Y., and Gaffey M. J. 2002. A critical evaluation of oxidation versus reduction during metamorphism of L and LL group chondrites, and implications for asteroid spectroscopy. *Meteoritics & Planetary Science* 37: 75–89.

Ghiorso M. S. and Sack R. O. 1995. Chemical mass transfer in magmatic processes IV. A revised and internally consistent thermodynamic model for the interpolation and extrapolation of liquid-solid equilibria in magmatic systems at elevated temperatures and pressures. *Contributions to Mineralogy and Petrology* 119:197–212.

Grady M. M. 2000. *Catalogue of meteorites: With special reference to those represented in the collection of the Natural History Museum, London, 5th edition.* London: Cambridge University Press. 689 p.

Gudmundsson G. and Holloway J. R. 1993. Activity-composition relationships in the system Fe-Pt at 1300 and 1400 °C and at 1 atm and 20 kbar. *American Mineralogist* 78:178–186.

Hashizume K. and Sugiura N. 1997. Isotopically anomalous nitrogen in H-chondrite metal. *Geochimica et Cosmochimica Acta* 61: 859–872.

Harvey R. P., Bennett M. L., and McSween H. Y. 1993. Pyroxene equilibration temperatures in metamorphosed ordinary chondrites (abstract). 24th Lunar and Planetary Science Conference. pp. 615–616.

Holland T. J. B. and Powell R. 1990. An enlarged and updated internally consistent thermodynamic data set with uncertainties and correlations: The system K_2O-Na_2O-CaO-MgO-MnO-FeO-Fe_2O_3-Al_2O_3-TiO_2-SiO_2-C-H_2-O_2. *Journal of Metamorphic Geology* 8:89–124.

Hsieh K. C., Vlach K. -C., and Chang Y. A. 1987. The Fe-Ni-S system I. A thermodynamic analysis of the phase equilibria and calculation of the phase diagram from 1173 to 1623 K. *High Temperature Science* 23:17–38.

Ikeda Y., Yamamoto T., Kojima H., Imae N., Kong P., Ebihara M., and Prinz M. 1997. Yamato-791093, a metal-sulfide-enriched H-group chondritic meteorite transitional to primitive IIE irons with silicate inclusions. *Antarctic Meteorite Research* 10:335–353.

Irvine T. N. 1965. Chromian spinel as a petrogenetic indicator. Part I. Theory. *Canadian Journal of Earth Sciences* 2:648–672.

Jackson E. D. 1969. Chemical variation in coexisting chromite and olivine in chromitite zones of the Stillwater complex. *Economic Geology Monograph* 4:41–71.

Jacob K. T. and Iyengar G. N. K. 1999. Thermodynamics and phase equilibria involving the spinel solid solution $Fe_xMg_{1-x}Cr_2O_4$. *Metallurgical and Materials Transactions* 30B:865–871.

Jarosewich E. 1990. Chemical analyses of meteorites: A compilation of stony and iron meteorite analyses. *Meteoritics* 25:323–337.

Johnson C. A. and Prinz M. 1991. Chromite and olivine in type II chondrules in carbonaceous and ordinary chondrites: Implications for thermal histories and group differences. *Geochimica et Cosmochimica Acta* 55:893–904.

Jönsson B. 1995. Assessment of the mobilities of Cr, Fe, and Ni in fcc Cr-Fe-Ni alloys. *Zeitschrift für Metallkunde* 86:686–692.

Keil K. and Fodor R. V. 1980. Origin and history of the polymict-

brecciated Tysnes Island chondrite and its carbonaceous and non-carbonaceous lithic fragments. *Chemie der Erde* 39:1–26.

Keil K. and Fredriksson K. 1964. The iron, magnesium, and calcium distribution in coexisting olivines and rhombic pyroxenes of chondrites. *Journal of Geophysical Research* 69: 3487–3515.

Kessel R., Beckett J. R., and Stolper E. M. 2001. Thermodynamic properties of the Pt-Fe system. *American Mineralogist* 86:1003–1014.

Kessel R., Beckett J. R., and Stolper E. M. 2002. The thermal history of equilibrated ordinary chondrites and the relationship between textural maturity and temperature. (abstract #1420). 33rd Lunar and Planetary Science Conference. CD-ROM

Kessel R., Beckett J. R., and Stolper E. M. 2003. Experimental determination of the activity of chromite in multicomponent spinels. *Geochimica et Cosmochimica Acta* 67:3033–3044.

Kessel R., Beckett J. R., and Stolper E. M. Forthcoming. The thermal history of equilibrated ordinary chondrites and the relationship between textural maturity and temperature. *Geochimica et Cosmochimica Acta.*

Kleinschrot D. and Okrusch M. 1999. Mineralogy, petrography, and thermometry of the H5 chondrite Carcote, Chile. *Meteoritics & Planetary Science* 34:795–802.

Klemme S., O'Neill H. St. C., Schnelle W., and Gmelin E. 2000. The heat capacity of $MgCr_2O_4$, $FeCr_2O_4$, and Cr_2O_3 at low temperatures and derived thermodynamic properties. *American Mineralogist* 85:1686–1693.

Larimer J. W. 1968. Experimental studies on the system Fe-MgO-SiO_2-O_2 and their bearing on the petrology of chondritic meteorites. *Geochimica et Cosmochimica Acta* 32:1187–1207.

Lauretta D. S., Buseck P. R., and Zega T. J. 2001. Opaque minerals in the matrix of the Bishunpur (LL3.1) chondrite: Constraints on the chondrule formation environment. *Geochimica et Cosmochimica Acta* 65:1337–1353.

Lindsley D. H. 1983. Pyroxene thermometry. *American Mineralogist* 68:477–493.

Mattioli G. S. and Wood B. J. 1986. Upper mantle oxygen fugacity recorded by spinel lherzolites. *Nature* 322:626–628.

Mattioli G. S., Wood B. J., and Carmichael I. S. E. 1987. Ternary-spinel volumes in the system $MgAl_2O_4$-Fe_3O_4-$\gamma Fe_{8/3}O_4$: Implications for the effect of P on intrinsic fO_2 measurements of mantle-xenolith spinels. *American Mineralogist* 72:468–480.

McSween H. Y. and Labotka T. C. 1993. Oxidation during metamorphism of the ordinary chondrites. *Geochimica et Cosmochimica Acta* 57:1105–1114.

McSween H. Y. and Patchen A. D. 1989. Pyroxene thermobarometry in LL-group chondrites and implications for parent body metamorphism. *Meteoritics* 24:219–226.

McSween H. Y., Sears D. W. G., and Dodd R. T. 1988. Thermal metamorphism. In *Meteorites and the early solar system,* edited by Kerridge J. F. and Matthews M. S. Tucson: University of Arizona Press. pp. 102–113.

Miettinen J. 1999. Thermodynamic reassessment of Fe-Cr-Ni system with emphasis on the iron-rich corner. *Calphad* 23:231–248.

Miyamoto M., Fujii N., and Takeda H. 1981. Ordinary chondrite parent body: An internal heating model. Proceedings, 12th Lunar and Planetary Science Conference. pp. 1145–1152.

Mueller R. F. 1964. Phase equilibria and the crystallization of chondritic meteorites. *Geochimica et Cosmochimica Acta* 28: 189–207.

Nafziger R. H. and Muan A. 1967. Equilibrium phase compositions and thermodynamic properties of olivines and pyroxenes in the system MgO-"FeO"-SiO_2. *American Mineralogist* 52:1364–1385.

Olsen E. J. and Bunch T. E. 1984. Equilibration temperatures of the ordinary chondrites: A new evaluation. *Geochimica et Cosmochimica Acta* 48:1363–1365.

Olsen E. J., Mayeda T. K., and Clayton R. N. 1981. Cristobalite-pyroxene in an L6 chondrite: Implications for metamorphism. *Earth and Planetary Science Letters* 56:82–88.

O'Neill H. St. C., Pownceby M. I., and McCammon C. A. 2003. The magnesiowüstite: Iron equilibrium and its implications for the activity-composition relations of $(Mg, Fe)_2SiO_4$ olivine solid solutions. *Contributions to Mineralogy and Petrology* 146:308–325.

Ozawa K. 1984. Olivine-spinel geospeedometry: Analysis of diffusion-controlled Mg-Fe^{2+} exchange. *Geochimica et Cosmochimica Acta* 48:2597–2611.

Petric A., Jacob K. T., and Alcock C. B. 1981. Thermodynamic properties of Fe_3O_4-$FeAl_2O_4$ spinel solid solutions. *Journal of the American Ceramic Society* 64:632–639.

Rambaldi E. R. and Wasson J. T. 1984. Metal and associated phases in Krymka and Chainpur: Nebular formational processes. *Geochimica et Cosmochimica Acta* 48:1885–1897.

Reuter K. B., Williams D. B., and Goldstein J. I. 1989. Determination of the Fe-Ni phase diagram below 400 °C. *Metallurgical Transactions* 20A:719–725.

Ringwood A. E. 1961. Chemical and genetic relationships among meteorites. *Geochimica et Cosmochimica Acta* 24:159–197.

Rubin A. E., Fegley B., and Brett R. 1988. Oxidation state in chondrites. In *Meteorites and the early solar system,* edited by Kerridge J. F. and Matthews M. S. Tucson: University of Arizona Press. pp. 488–511.

Sack R. O. and Ghiorso M. S. 1991a. An internally consistent model for the Thermodynamic properties of Fe-Mg-titanomagnetite-aluminate spinels. *Contributions to Mineralogy and Petrology* 106:474–505.

Sack R. O. and Ghiorso M. S. 1991b. Chromian spinels as petrogenetic indicators: Thermodynamics and petrological applications. *American Mineralogist* 76:827–847.

Senderov E., Dogan A. U., and Navrotsky A. 1993. Nonstoichiometry of magnetite-ulvöspinel solid solutions quenched from 1300 °C. *American Mineralogist* 78:565–573.

Snetsinger K. G., Keil K., and Bunch T. E. 1967. Chromite from "equilibrated" chondrites. *American Mineralogist* 52:1322–1331.

Sugimoto W., Kaneko N., Sugahara Y., and Kuroda K. 1997. Preparation of stoichiometric and nonstoichiometric magnesium titanate spinels. *Journal of the Ceramic Society of Japan* 105: 101–105.

Thy P., Lofgren G. E., and Imsland P. 1991. Melting relations and the evolution of the Jan Mayen magma system. *Journal of Petrology* 32:303–332.

Van Schmus W. R. 1969. The mineralogy and petrology of chondritic meteorites. *Earth Science Reviews* 5:145–184.

Van Schmus W. R. and Wood J. A. 1967. A chemical-petrologic classification for the chondritic meteorites. *Geochimica et Cosmochimica Acta* 31:747–765.

Virgo D., Luth R. W., Moats M. A., and Ulmer G. C. 1988. Constraints on the oxidation state of the mantle: An electrochemical and ^{57}Fe Mössbauer study of mantle-derived ilmenites. *Geochimica et Cosmochimica Acta* 52:1781–1794.

Von Seckendorff V. and O'Neill H. St. C. 1993. An experimental study of Fe-Mg partitioning between olivine and orthopyroxene at 1173, 1273, and 1423 K and 1.6 GPa. *Contributions to Mineralogy and Petrology* 113:196–207.

Walter L. S. and Doan A. S. 1969. Determination of oxygen activities of chondritic meteorites. *Geological Society of America Abstracts with Programs* 1:232–233.

Wetherill G. W. and Chapman C. R. 1988. Asteroids and meteorites.

In *Meteorites and the early solar system,* edited by Kerridge J. F. and Matthews M. S. Tucson: University of Arizona Press. pp. 35–67.

Wilkison S. L. and Robinson M. S. 2000. Bulk density of ordinary chondrite meteorites and implications for asteroidal internal structure. *Meteoritics & Planetary Science* 35:1203–1213.

Williams R. J. 1971a. Reaction constants in the system Fe-MgO-SiO_2-O_2 at 1 atm between 900° and 1300 °C: Experimental results. *American Journal of Science* 270:334–360.

Williams R. J. 1971b. Equilibrium temperatures, pressures, and oxygen fugacities of the equilibrated chondrites. *Geochimica et Cosmochimica Acta* 35:407–411.

Willis J. and Goldstein J. I. 1983. A three-dimensional study of metal grains in equilibrated, ordinary chondrites. Proceedings, 14th Lunar and Planetary Science Conference. *Journal of Geophysical Research* 88:B287–B292.

Wiser N. M. and Wood B. J. 1991. Experimental determination of activities in Fe-Mg olivine at 1400 K. *Contributions to Mineralogy and Petrology* 108:146–153.

Wlotzka F. and Fredriksson K. 1980. Morro de Rocio, an unequilibrated H5 chondrite. *Meteoritics* 15:387–388.

Young E. D. 2001. The hydrology of carbonaceous chondrite parent bodies and the evolution of planet progenitors. *Philosophical Transactions of the Royal Society of London A* 359:2095–2110.

Zanda B., Bourot-Denise M., Perron C., and Hewins R. H. 1994. Origin and metamorphic redistribution of silicon, chromium, and phosphorus in the metal of chondrites. *Science* 265:1846–1849.

Zinovieva N. G., Mitreikina O. B., and Granovsky L. B. 1997. Origin mechanism of hercynite-kamacite objects: Evidence for liquid immiscibility phenomena in the Yamato-82133 ordinary chondrite (H3). *Antarctic Meteorite Research* 10:299–311.